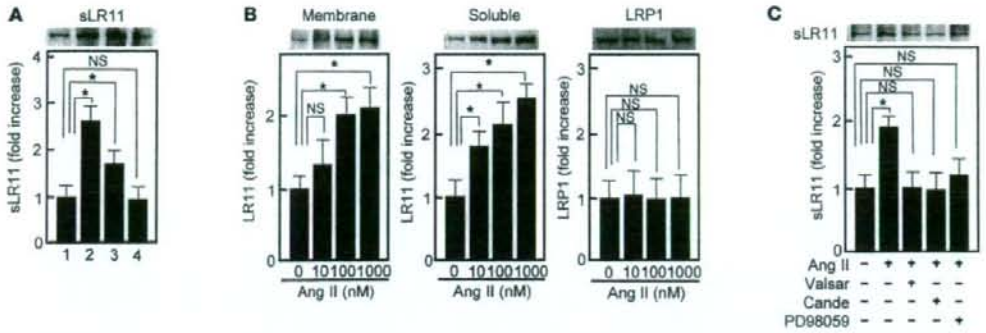

Figure 8
Ang II–induced sLR11 production in SMCs. (**A**) Effects of chemotactic cytokines on the production of sLR11 in rabbit SMCs. Conditioned media collected for 12 hours in the absence (lane 1) or presence of Ang II (1 μM, lane 2), PDGF (10 ng/ml, lane 3), or VEGF (50 ng/ml, lane 4) were concentrated and subjected to immunoblot analysis using anti-LR11 antibody (~250 kDa). Blot shown is representative of 3 independent experiments. Data are presented as mean ± SD (n = 3). *P < 0.05. (**B**) Ang II–dependent increase of soluble or membrane-bound forms of LR11 in SMCs. Membrane extracts (20 μg protein) prepared from rabbit SMCs or conditioned medium collected for 12 hours after the addition of Ang II at the indicated concentrations were subjected to immunoblot analysis with anti-LR11 (~250 kDa) or anti-LRP1 (~85 kDa) antibody. Blot shown is representative of 3 independent experiments. Data are presented as mean ± SD (n = 3). (**C**) Effect of ARBs or an ERK inhibitor on the Ang II–dependent increase in sLR11 in rabbit SMCs. Conditioned medium collected for 12 hours in the presence or absence of Ang II with or without valsartan (valsar, 10 nM), candesartan (10 nM), or PD98059 (10 μM) were subjected to immunoblot analysis with anti-LR11 (~250 kDa) antibody. Blot shown is representative of 3 independent experiments. Data are presented as mean ± SD (n = 3).

various diseases accompanied with vascular damage needs to be evaluated in future studies.

It is of interest that in the central nervous system, LR11 directs trafficking of amyloid precursor protein into recycling pathways (39) and LR11 expression is reduced in sporadic Alzheimer disease (40). We have recently shown that inherited *LR11/SORL1* variants are associated with late-onset Alzheimer disease (39). Furthermore, soluble circulating LRP1 has been shown to provide key endogenous peripheral "sink" activity for amyloid β-peptide in humans (41). The functions of LR11 in amyloid precursor protein and uPAR catabolism in association with LRP1 suggest multiple roles for LR11 in the degradation and/or transport of several cell-surface and cytoplasmic molecules. In any case, the vascular phenotype of LR11 deficiency, i.e., severely disturbed Ang II–mediated migration of SMCs through decreased uPAR catabolism, provides a system for studies on the regulation of vascular remodeling toward the development of novel therapeutic interventions.

Methods

Subjects. The study subjects are participants in a cohort study carried out concurrently with health-check screening at Awa area in Chiba, Japan (42). From among the 22,228 participants screened initially, we selected individuals with dyslipidemia (LDL cholesterol [LDL-C] > 160 mg/dl, triglycerides > 200 mg/dl, or HDL-cholesterol [HDL-C] < 35 mg/dl). None of the selected participants had medical complications or was undergoing treatment for abnormal plasma lipids, glucose, or blood pressure levels. The selected participants visited a hospital for detailed examination of their clinical profiles, collection of fasting blood samples, and measurement of carotid IMT. None had diabetes mellitus or thyroid and endocrinological diseases. All gave written informed consent prior to the study, which was approved by the Human Investigation Review Committee of the Chiba University Graduate School of Medicine. Examination of IMT was carried out with an ultrasound scanner (SSD-1200CV; ALOKA) equipped with a linear 7.5-MHz transducer (32, 43). IMT was defined as the distance from the leading edge of the lumen-intima interface to the leading edge of the media-adventitia interface of the far wall. The measurement of IMT in the common carotid artery was made along a 10-mm section just proximal to the carotid bulb (32, 43), and the average IMT was calculated from the right and left IMTs of common carotid arteries. Venous blood was drawn after an overnight fast of 12–14 hours. Serum was separated from blood cells by centrifugation and used for the measurement of lipids and other biochemical markers (2). LDL-C was estimated with the equation of Friedewald (32). LDL particle size and malondialdehyde-LDL levels were determined using gradient gel electrophoresis and sandwich ELISA, respectively (32). sLR11 was immunologically measured as described in Immunoblotting and immunoprecipitation.

Generation of Lr11$^{-/-}$ mice. A plasmid-targeting vector was constructed with 3.3 kb (5′) and 4.4 kb (3′) of genomic DNA flanking the neomycin resistance cassette (*Neo*^{r}) to target the first exon of murine LR11. After linearization, the plasmid was introduced into 129/Sv-derived embryonic stem cells by electroporation. Homologous recombinants were identified, and 2 independently targeted clones were injected into C57BL/6 blastocysts to generate chimeric mice. Male chimeras were crossbred with C57BL/6 females, and germline transmission was verified by Southern blot analysis. For Southern blot analysis, genomic DNA was prepared from the tail and digested with *Eco*RV. The fragments were separated by electrophoresis, transferred to a membrane, and hybridized with specific fragments corresponding to flanking regions of homologous recombination as probes for the identification of *Lr11*$^{+/+}$, *Lr11*$^{+/-}$, and *Lr11*$^{-/-}$ mice, as described previously (44). All animal studies were

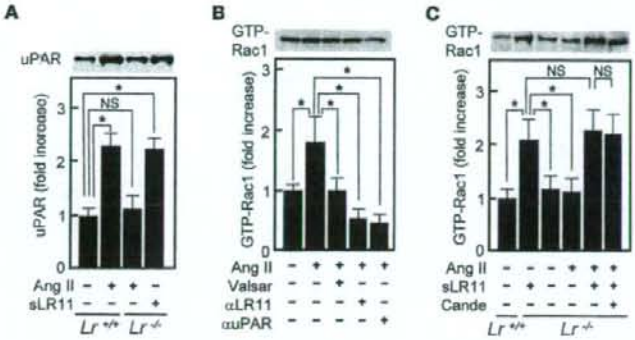

Figure 9

Ang II–induced LR11/uPAR pathway in SMCs. (**A**) uPAR expression in *Lr11*$^{-/-}$ SMCs. Membrane extracts of *Lr11*$^{+/+}$ SMCs or *Lr11*$^{-/-}$ SMCs were incubated with or without Ang II (1 μM) in the presence or absence of sLR11 (1 μg/μl) and subjected to immunoblot analysis using anti-uPAR (–50 kDa) antibody. Blot shown is representative of 3 independent experiments. Data are presented as mean ± SD (n = 3). *P < 0.05. (**B**) Effect of blocking the LR11/uPAR pathway on the Ang II–dependent increase of Rac1 activation in rabbit SMCs. Cell lysates (60 μg protein) were incubated in the presence or absence of Ang II (1 μM) with or without valsartan (10 nM), anti-LR11 antibody, or anti-uPAR antibody, immunoprecipitated with PAK-1 PBD Protein GST beads, and subjected to immunoblot analysis using anti-Rac1 (~21 kDa) antibody. Blot shown is representative of 3 independent experiments. Data are presented as mean ± SD (n = 3). (**C**) Effect of ARB on the Ang II–dependent increase of Rac1 activation in *Lr11*$^{-/-}$ SMCs. Cell lysate (60 μg protein) of *Lr11*$^{+/+}$ or *Lr11*$^{-/-}$ SMCs was incubated in the presence or absence of Ang II (1 μM) with or without candesartan (10 nM) or sLR11 (1 μg/μl), immunoprecipitated with PAK-1 PBD Protein GST beads, and subjected to immunoblot analysis using anti-Rac1 (~21 kDa) antibody. Blot shown is representative of 3 independent experiments. Data are presented as mean ± SD (n = 3).

approved by the Special Committee on Animal Welfare, School of Medicine, at the Inohana Campus of Chiba University.

Vascular injury by cuff placement. Cuff-placement surgery was carried out on 20-week-old male mice, as described (11). After isolating the right femoral artery from the surrounding tissues, a polyethylene tube (2-mm PE-90; BD) was opened longitudinally, loosely placed around the artery, and then closed with sutures. These arteries were removed from mice after 4 weeks; this was followed by serial perfusion with PBS(–) and with 10% neutral buffered formalin at 100 mmHg. The tissue was fixed in 10% neutral buffered formalin overnight, dehydrated, and embedded in paraffin. The middle segment of the artery was cut into subserial 5-μm cross sections with an interval of 50 μm between them. The sections were stained with elastica van Gieson or used for subsequent histochemical analyses. The image analysis software WinROOF (Mitani Corp.) was used to measure the areas of the intima and the media, respectively.

Laser capture microdissection. Frozen samples of cuffed artery were immediately embedded in OCT medium (Tissue-Tek; QIAGEN) and allowed to equilibrate to the cryostat temperature of –20°C. Each sample was sectioned into 10-μm specimens, placed on slides (Arcturus; Molecular Devices), and directly fixed in fresh 95% ethanol. After complete dehydration, the slides were placed in solutions of 75% ethanol for 30 seconds, 95% ethanol for 30 seconds, 100% ethanol for 30 seconds, and xylene for 5 minutes, then allowed to dry. SMCs in intimal and medial layers were captured for subsequent RNA experiments using a PixCell II Laser Capture Microdissection System (Molecular Devices).

Ang II infusion. The surgical procedures for connection to ALZET osmotic minipumps were performed together with those for cuff placement in *Lr11*$^{+/+}$ and *Lr11*$^{-/-}$ mice. The pumps delivered either saline or Ang II at a rate of 1 μg/kg per minute. The arteries were removed from mice after 4 weeks.

Antibodies, recombinant proteins, and ARBs. Mouse monoclonal (5-4-30-19-2) and rabbit polyclonal (pm11) antibodies against LR11 were described previously (11). Polyclonal antibodies against uPAR (AP807), NMHCII-B (PRB-445P), integrin αV (RMV-7), GST (A-30), and (phospho-) p44/42 MAP kinase and (phospho-) Stat1 were from R&D Systems, Covance, BioLegend, BostonBiochem, and Cell Signaling Technology, respectively. Monoclonal antibodies against LRP1, SMA (1A4), FAK (MAb2A7), p-Y397 of FAK, and integrin αvβ3 (MAB1976) were from Research Diagnostics Inc., Dako, Upstate Biotechnology (Millipore), BioSource (Invitrogen), and Chemicon (Millipore), respectively. Recombinant PDGF-BB, angiotensin II, VEGF, and plasmin were from R&D Systems, Sigma-Aldrich, Wako, and American Diagnostica, respectively. apoE and 39-kDa RAP were from Cosmo Bio Co. Ltd. Recombinant sLR11 protein lacking the 104 C-terminal amino acids containing the transmembrane region (sLR11) was prepared as described (20). Purified sLR11 was used for experiments at a concentration of 1 μg/ml, estimated from its biological activity in stimulating the migration of rabbit SMCs. The ARBs valsartan (CGP48933) and candesartan (CV-11974) were obtained from Novartis and Takeda Pharmaceutical Co. Ltd., respectively.

Cells. Primary cultures of mouse SMCs were prepared as described (45). In brief, the whole aortae prepared from 10-week-old mice were cut into pieces of approximately 1 mm^2 after removal of adventitial connective tissue and luminal endothelial cells. The pieces were digested with 1 mg/ml collagenase (Nitta Gelatin Inc.) and 20 U/ml elastase (Elastin Products Co. Inc.) in DMEM (Sigma-Aldrich) for 30 minutes at 37°C, and centrifuged at 2,000 g for 10 minutes at 4°C. The precipitate was resuspended in DMEM supplemented with 10% FBS (GIBCO; Invitrogen) and 40 μg/ml gentamycin (Schering-Plough). After 2 to 10 passages, cells from the primary culture were used for experiments. Primary cultures of rabbit SMCs were prepared from the medial layers of aortae as described (13) and used at passages 3 and 4. The LR11-overexpressing A7r5 cells (a rat embryonic aortic SMC line), R-1, and the control line C-1 were established as described (13). Before migration, biochemical, and immunological assays, cells were preincubated with various agents under the

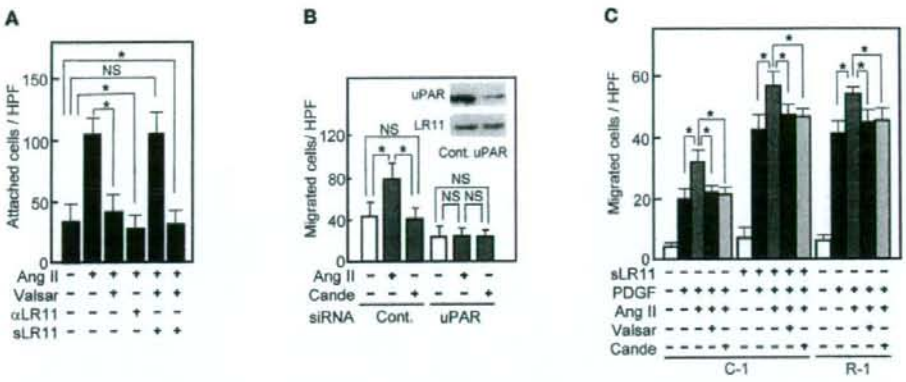

Figure 10

Ang II–induced migration via the LR11/uPAR pathway in SMCs. (**A**) Effect of blocking LR11 activation on the Ang II–induced increase of attachment of rabbit SMCs. The SMCs attached to plastic plates were counted after incubation in the presence or absence of Ang II (1 μM) with or without valsartan (10 nM), anti-LR11 antibody, or sLR11 (1 μg/μl). Data are presented as mean ± SD ($n = 3$). *$P < 0.05$. (**B**) Effect of uPAR silencing on the Ang II–induced increase in rabbit SMCs migration. The migrated SMCs treated with exogeneous siRNA specific for uPAR or control (Cont.) RNA were counted after incubation in the presence or absence of Ang II (1 μM) with or without candesartan (10 nM). Inset: Membrane extracts (10 μg protein) prepared from these cells were subjected to immunoblot analysis with anti-uPAR (~50 kDa) or anti-LR11 antibody (~250 kDa). Data are presented as mean ± SD ($n = 3$). (**C**) Effect of Ang II on the PDGF-induced migration of LR11-overexpressing SMCs. The number of migrated A7r5 cells transfected with LR11 cDNA (R-1), or control cells (C-1) in the presence or absence of PDGF-BB (PDGF, 10 ng/ml) were determined after incubation with or without sLR11 (1 μg/μl), Ang II (1 μM), or valsartan (10 nM). Data are presented as mean ± SD ($n = 10$).

conditions indicated in the figure legends at 37°C, and then aliquots of the cell suspension were used for the experiments.

RT-PCR. Total RNA was purified from the microdissected or cultured cells using an RNeasy kit (QIAGEN) as described (11). The methods for RT-PCR have been described (46). The amplified products were visualized after gel electrophoresis. For quantification of transcript levels, real-time PCR was performed using SYBR Green PCR master mix (Applied Biosystems). The sequences of the PCR primers were according to known cDNA sequences: LR11, 5′-AATGGTGTTTGGTTGAAACACACATCT-TAG-3′ and 5′-TACGTGGTTTCAACTACCAGAAATGCGCTT-3′; LRP1, 5′-CGGAACTGTACCATTTCA-3′ and 5′-GGTGTTGACAACCCATTCG-3′; NMMHCII-B, 5′-TGGAGCATCCCGAGAGGTATCT-3′ and 5′-GGAATCCACACCAGCTTTTTAGC-3′; SM1, 5′-CTCAAGAGCAAACT-CAGGAG-3′ and 5′-TCTGTGACTTGAGAACGAAT-3′; β-actin, 5′-AGAGGGAAATCGTGCGTGAC-3′ and 5′-CAATAGTGATGACCTG-GCCGT-3′. mRNA amounts were normalized to levels of β-actin mRNA, which served as the internal standard.

Migration, invasion, attachment, and proliferation assays. Cell migration and invasion were measured essentially as previously described (13), using a 96-well micro-Boyden chamber, its surface coated with type I collagen, and Transwell (Corning) 24-well plates coated with 100 μl collagen gel, respectively. The lower chamber contained 1% FBS-DMEM with or without 10 ng/ml PDGF-BB. After a 4-hour incubation at 37°C, the cells on the upper surfaces were washed, fixed, and stained by Diff-Quik (International Reagents Corp.). The number of cells that migrated to the lower (outer) surface of the filters (high-power field) was determined microscopically by counting. Cell adhesion was determined in a 96-well plate, the surface of which was coated with type I collagen, as described (20). After a 2-hour incubation at 37°C, nonadherent cells were removed by gently washing with PBS and adherent cells were determined by counting. Cell proliferation was measured based on the incorporation of BrdU during DNA synthesis of proliferating cells using a cell proliferation ELISA system (Amersham). In brief, after 48-hour incubation at 37°C without FBS, SMCs (8,000 cells/well) were labeled with BrdU (10 μmol/l) in the presence or absence of Ang II for 8 hours. DNA synthesis was assessed by measuring the amount of BrdU incorporation into the DNA, which was detected by the above immunoassay system.

Immunoblotting and immunoprecipitation. Cultured cells were washed 3 times with PBS and harvested in PBS containing 0.5 mM PMSF and 2.5 μM leupeptin. The pellet after ultracentrifugation at 100,000 *g* for 1 hour was resuspended in solubilization buffer (200 mM Tris-maleate, pH 6.5, 2 mM $CaCl_2$, 0.5 mM PMSF, 2.5 μM leupeptin, and 1% Triton X-100) as previously described (11). Conditioned medium was concentrated 20-fold using Centricon-100 concentrators (Millipore) (5). 50 ml of serum was purified using a RAP-GST affinity column. For immunoblotting, equal amounts of membrane protein, protein extracted from pelleted beads, or concentrated medium were subjected to 10% SDS-PAGE after heating to 95°C for 5 minutes as described (47) under reducing conditions and transferred to a nitrocellulose membrane. Incubations were with antibody against LR11 (5-4-30-19-2, 1:500 dilution; or pm11, 1:200 dilution), LRP1 (1:500 dilution) (phospho-) p44/42 MAP kinase (1:1000 dilution) (phospho-) Stat1 (1:500 dilution), Rac1 (1:1000 dilution), integrin αvβ3 (MAB1976, 1:1000 dilution), or uPAR (1:500 dilution) followed by peroxidase-conjugated anti-mouse, anti-rabbit, or anti-goat IgG. For immunoprecipitation, 100 μg of membrane protein was mixed with sLR11 (1 μg/μl) at 4°C for 3 hours in the presence or absence of apoE (50 μg) or RAP (10 μg), as indicated in Figure 6B. The LR11/uPAR/integrin/antibody complex was precipitated by protein A-Sepharose. The proteins were released into 25 μl SDS sample buffer by heating to 95°C for 5 minutes. For immunodetection, pm11 (1:200 dilution) was used, followed by peroxidase-conjugated anti-rabbit IgG. Development was performed with the ECL detection reagents (Amersham). The signals were quantified by densitometric scanning using NIH Image software. The sLR11 level of each subject's serum (50 μl) was determined in a blinded manner as an averaged value of 3 quantified signal

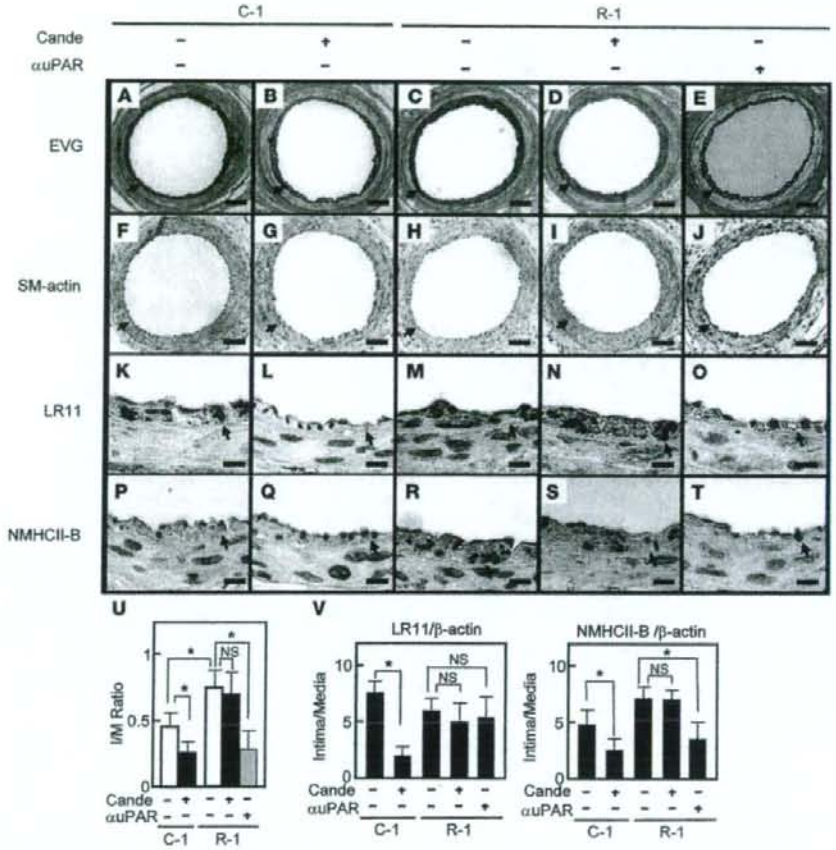

Figure 11

Effect of the ARB candesartan on intimal thickness after arterial injury in sLR11-overproducing mice. BL6 nude mice were implanted subcutaneously with A7r5 cells transfected with LR11 cDNA (R-1) or control cells (C-1). Sections of femoral arteries of cell-implanted mice after cuff placement with or without administration of candesartan or anti-uPAR neutralizing antibody were subjected to histological analysis using elastica van Gieson (EVG) staining (**A–E**). Serial sections were immunohistochemically analyzed using antibody against SMA (**F–J**), LR11 (**K–O**), or NMHCII-B (**P–T**). Arrowheads indicate the internal elastic layers. Scale bars: 50 μm (**A–J**); 10 μm (**K–T**). (**U**) I/M ratio of arteries is presented as mean ± SD ($n = 5$). *$P < 0.05$. (**V**) mRNA levels of LR11 and NMHCII-B in injured arteries. Total RNA isolated from thickened intima or media of mice using LCM was reverse transcribed and subjected to real-time PCR analysis using specific primers for NMHCII-B and LR11, respectively. The amounts of amplified products are expressed relative to the amounts of β-actin transcript, and the ratio of mRNA expression levels of intima and media are presented as mean ± SD ($n = 3$).

intensities resulting from independent assays and expressed as a ratio to that of a standard serum. The immunological estimation indicated that the signal of 1 U (in 50 μl serum) corresponded to approximately 50 ng/ml of recombinant sLR11. For analysis of phosphorylated ERK, Rac1 pull-down, and FAK phosphorylation, cells were starved for 24 hours in 0.3% FBS-DMEM followed by the addition of sLR11 (1 μg/ml) for the indicated times in the presence or absence of anti-integrin antibody (MAB1976 or RMV-7, 1:200 dilution) as described (13). For Rac1 pull-down and FAK phosphorylation assays, cells were lysed directly in the plates with ice-cold magnesium-containing lysis buffer and RIPA buffer, respectively. GTP-Rac1 activity was measured with a PAK-1 PBD/Rac activation assay kit (Upstate Biotechnology). In brief, lysates were incubated at 4°C with 10 μg of PAK-1 PBD Protein GST beads for 60 minutes. The proteins were released into 25 μl SDS sample buffer by heating to 95°C for 5 minutes. For FAK phosphorylation measurement after immunoprecipitation with antibody against FAK (MAb2A7), lysates were subjected to electrophoresis in 7.5% SDS gels and transferred to nitrocellulose membranes. The membranes were probed with an antibody specific for FAK-pY397 (1:1000) and then reprobed with an anti-FAK antibody (MAb2A7, 1:500).

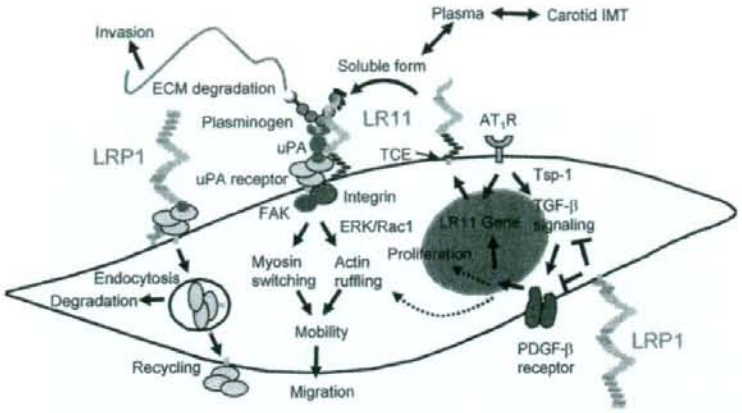

Figure 12
Proposed molecular mechanism for LR11 requirement in the response of SMCs to Ang II. Ang II and PDGF-BB are the key cytokines promoting migration of SMCs in plaque formation. LRP1 inhibits the PDGF-BB–mediated signals for migration and proliferation and/or the modulation of upstream Tsp-1/TGF-β–mediated signals (38) through interaction with the PDGF-β receptor. Ang II induces the Tsp-1/TGF-β signals (37) and LR11 gene transcription through activating AT_1R. LR11 localized on the cell surface becomes the soluble form (as sLR11) by cleavage through TNF-α–converting enzyme (TCE) (22). Circulating sLR11 levels are positively correlated with carotid IMT. sLR11 binds to and interacts with uPAR, the expression of which is mainly regulated by LRP1, on the cell surface and/or on neighboring cells. This complex formation inhibits the internalization of uPAR via LRP1, resulting in enhanced uPAR cell-surface expression. The uPA/uPAR system increases cell mobility through both increased ECM degradation and intracellular integrin/FAK/ERK/Rac-1 signaling, which in turn promotes actin ruffling and myosin isoform switching. The SMCs expressing LR11 display increased migratory capacity in response to PDGF-BB and/or Ang II. Thus, LR11 in combination with its counteracting partner LRP1 regulates the migration of intimal SMCs in injured arteries and atherosclerotic plaques via modulation of the uPA/uPAR system. The proposed LR11-mediated migration of intimal SMCs may be modulated by other Ang II–induced molecules and cytokines, particularly endothelial cell–derived PAI-1 (48). ARBs inhibit (a) the migration of intimal SMCs through downregulation of LR11 and (b) their proliferation by blockade of signals mediated by Tsp-1/TGF-β and PDGF-BB.

Transfection of SMCs with siRNA. Oligonucleotides were synthesized for siRNA (Takara Bio Inc.). Annealed sense and antisense oligonucleotides (25 nM each), 5′-UGGCUUCCAAUGUUACAGCTT-3′ and 5′-GCUGUAACAUUGGAAGCCATT-3′ corresponding to the uPAR sequence, or 5′-GAUGCCAUCUGUAGUCACUTT-3′ and 5′-AGUGACUACAGAUGGCAUCTT-3′ for control were transfected into SMCs (1×10^6 cells/100 mm dish) and incubated for 2 days as described (14). Cells were then used for experiments.

Immunohistochemistry. Serial paraffin-embedded sections (5 μm) were used for immunohistostaining as described (11). Deparaffinized sections were pretreated with 0.3% H_2O_2 to inactivate endogenous peroxidase. Slides were stained in the presence of 3% BSA with antibody against LR11 (pm11, 1:50 dilution), NMHCII-B (1:100 dilution), or SMA (1:1 dilution) at 23°C for 1 hour followed by HRP-conjugated anti-rabbit IgG secondary antibodies (Molecular Probes) at 1:200 dilution. The slides were counterstained with hematoxylin. Controls with nonimmune rabbit IgG were conducted in parallel with each immunoassay procedure.

Immunofluorescence. Cells were grown to 70% confluence on LabTek chamber slides (Nunc). For assays of membrane ruffling, cells were preincubated with PDGF-BB (10 ng/ml), Ang II (1 μM), sLR11 (1 μg/ml), anti-LR11 antibody (pm11, 1:5 dilution), anti-uPAR antibody (10 μg/ml), anti-integrin αvβ3 antibody (10 μg/ml), or PD98059 (10 μM; Calbiochem) for the indicated times. Cells were fixed in 4% paraformaldehyde in PBS at 4°C for 15 minutes, as described (11). F-actin was labeled using Alexa Fluor 488 phalloidin (1:40 dilution, A12379; Invitrogen) for measurement of ruffle formation. Slides were examined with a Zeiss LSM5 PASCAL confocal laser scanning microscope. The 488-nm line of the argon laser was used for excitation of Alexa Fluor 488. The number of cells with membrane ruffling were counted with 500 cells in the field.

sLR11-overproducing mouse model. R-1 and C-1 cells were grown to near confluence, trypsinized, and suspended in DMEM with 10% FBS. After centrifugation, cell pellets were resuspended in PBS. Eight-week-old ICR nude mice were injected subcutaneously with either 1×10^7 R-1 cells or C-1 cells. The injection through 21-gauge needles into subcutaneous areas of nude mice was performed under anesthesia, as described (23). The surgical operations for cuff placement and connection to a supply osmotic minipump for candesartan (0.1 mg/kg/day) followed 4 weeks after cell implantations. Polyclonal antibodies against uPAR (1:500 dilution) or against GST (control, 1:200 dilution) in PBS were injected intraperitoneally, in each case 2–3 days after cuff treatment of mice injected with R-1 cells. Blood samples were collected for the immunodetection of sLR11. Six weeks after cell implantation, the femoral arteries were recovered for immunohistological analyses.

Statistics. Statistical analysis was performed with SPSS version 13.0 (SPSS Japan Inc.). Associations of IMT or sLR11 levels with risk factors were examined by Pearson correlation analysis for continuous variables and by unpaired *t* test for categorical variables between groups (sex and smoking) (see Supplemental Table 2). Subsequently, multiple linear regression analyses were used to calculate the ORs for the IMT for Table 1 (a) by controlling for age, blood pressure, and HDL-C, which are significantly correlated with IMT, with $P < 0.001$ by above analyses (model 1); and (b) by additionally controlling for all risk factors (age, sex, BMI, blood pressure, smoking, LDL-C, HDL-C, triglycerides, LDL size, malondialdehyde-LDL, glucose, and insulin) used for the above analyses (model 2). Finally, the ORs were calculated for the IMT with raised baseline sLR11 (second, third, and fourth quartiles) compared with low baseline sLR11 (lowest quartile) by controlling for age. In the figures, the results are shown as mean ± SD for each index. 1-way ANOVA was used to compare between 2 groups, and Duncan's multiple-range test was used for comparison of multiple groups. A value of $P < 0.05$ was considered significant.

Acknowledgments

These studies were supported by grants from the Japanese Ministry of Education, Culture, Sports, Science and Technology (to Y. Saito and H. Bujo), the Austrian Science Foundation (FWF), and the Herzfelder'sche family endowment (to W.J. Schneider).

Received for publication April 11, 2007, and accepted in revised form May 21, 2008.

Address correspondence to: Hideaki Bujo, Department of Genome Research and Clinical Application, Chiba University Graduate School of Medicine, 1-8-1 Inohana, Chuo-ku, Chiba 260-8670, Japan. Phone: 81-43-222-7171; Fax: 81-43-226-2095. E-mail: hbujo@faculty.chiba-u.jp. Or to: Wolfgang J. Schneider, Department of Medical Biochemistry, Medical University of Vienna, Dr. Bohr Gasse 9/2, A-1030 Vienna, Austria. Phone: 43-1-4277-61803; Fax: 43-1-4277-61804. E-mail: wolfgang.schneider@meduniwien.ac.at.

1. Ross, R. 1999. Atherosclerosis — an inflammatory disease. *N. Engl. J. Med.* **340**:115–126.
2. Newby, A.C. 2005. Dual role of matrix metalloproteinases (matrixins) in intimal thickening and atherosclerotic plaque rupture. *Physiol. Rev.* **85**:1–31.
3. Blasi, F., and Carmeliet, P. 2002. uPAR: a versatile signalling orchestrator. *Nat. Rev. Mol. Cell. Biol.* **3**:932–943.
4. Reuning, U., Magdolen, V., Hapke, S., and Schmitt, M. 2003. Molecular and functional interdependence of the urokinase-type plasminogen activator system with integrins. *Biol. Chem.* **384**:1119–1131.
5. Herz, J., and Hui, D.Y. 2004. Lipoprotein receptors in the vascular wall. *Curr. Opin. Lipidol.* **15**:175–181.
6. Gonias, S.L., Wu, L., and Salicioni, A.M. 2004. Low density lipoprotein receptor-related protein: regulation of the plasma membrane proteome. *Thromb. Haemost.* **91**:1056–1064.
7. Bujo, H., and Saito, Y. 2006. Modulation of smooth muscle cell migration by members of the low-density lipoprotein receptor family. *Arterioscler. Thromb. Vasc. Biol.* **26**:1246–1252.
8. Yamazaki, H., et al. 1996. Elements of neural adhesion molecules and a yeast vacuolar protein sorting receptor are present in a novel mammalian low density lipoprotein receptor family member. *J. Biol. Chem.* **271**:24761–24768.
9. Jacobsen, L., et al. 1996. Molecular characterization of a novel human hybrid-type receptor that binds the α_2-macroglobulin receptor associated protein (RAP). *J. Biol. Chem.* **271**:31379–31383.
10. Morwald, S., et al. 1997. A novel mosaic protein containing LDL receptor elements is highly conserved in humans and chickens. *Arterioscler. Thromb. Vasc. Biol.* **17**:996–1002.
11. Zhu, Y., et al. 2004. LR11, an LDL receptor gene family member, is a novel regulator of smooth muscle cell migration. *Circ. Res.* **94**:752–758.
12. Kanaki, T., et al. 1999. Expression of LR11, a mosaic LDL receptor family member, is markedly increased in atherosclerotic lesions. *Arterioscler. Thromb. Vasc. Biol.* **19**:2687–2695.
13. Zhu, Y., et al. 2002. Enhanced expression of the LDL receptor family member LR11 increases migration of smooth muscle cells in vitro. *Circulation.* **105**:1830–1836.
14. Jiang, M., et al. 2006. Pitavastatin attenuates the PDGF-induced LR11/uPA receptor-mediated migration of smooth muscle cells. *Biochem. Biophys. Res. Commun.* **348**:1367–1377.
15. Xi, X.P., et al. 1999. Central role of the MAPK pathway in AngII-mediated DNA synthesis and migration in rat vascular smooth muscle cells. *Arterioscler. Thromb. Vasc. Biol.* **19**:73–82.
16. Nickenig, G., and Harrison, D.G. 2002. The AT_1-type angiotensin receptor in oxidative stress and atherogenesis: part I: oxidative stress and atherogenesis. *Circulation.* **105**:393–396.
17. Zuo, L., et al. 2005. Caveolin-1 is essential for activation of Rac1 and NAD(P)H oxidase after angiotensin II type 1 receptor stimulation in vascular smooth muscle cells: role in redox signaling and vascular hypertrophy. *Arterioscler. Thromb. Vasc. Biol.* **25**:1824–1830.
18. Horiuchi, M., et al. 2003. Fluvastatin enhances the inhibitory effects of a selective angiotensin II type 1 receptor blocker, valsartan, on vascular neointimal formation. *Circulation.* **107**:106–112.
19. O'Leary, D.H., et al. 1999. Carotid-artery intima and media thickness as a risk factor for myocardial infarction and stroke in older adults. Cardiovascular Health Study Collaborative Research Group. *N. Engl. J. Med.* **340**:14–22.
20. Ohwaki, K., et al. 2007. A secreted soluble form of LR11, specifically expressed in intimal smooth muscle cells, accelerates formation of lipid-laden macrophages. *Arterioscler. Thromb. Vasc. Biol.* **27**:1050–1056.
21. Manabe, I., and Nagai, R. 2003. Regulation of smooth muscle phenotype. *Curr. Atheroscler. Rep.* **5**:214–222.
22. Hermey, G., Sjogaard, S.S., Petersen, C.M., Nykjaer, A., and Gliemann, J. 2006. Tumour necrosis factor alpha-converting enzyme mediates ectodomain shedding of Vps10p-domain receptor family members. *Biochem. J.* **395**:285–293.
23. Kitagawa, Y., et al. 2004.Impaired glucose tolerance is accompanied by decreased insulin sensitivity in tissues of mice implanted with cells that overexpress resistin. *Diabetologia.* **47**:1847–1853.
24. Trommsdorff, M., et al. 1999. Reeler/Disabled-like disruption of neuronal migration in knockout mice lacking the VLDL receptor and ApoE receptor 2. *Cell.* **97**:689–701.
25. Webb, D.J., Nguyen, D.H.D., Sankovic, M., and Gonias, S.L. 1999. The very low density lipoprotein receptor regulates urokinase receptor catabolism and breast cancer cell motility in vitro. *J. Biol. Chem.* **274**:7412–7420.
26. Webb, D.J., Nguyen, D.H.D., and Gonias, S.L. 2000. Extracellular signal-regulated kinase functions in the urokinase receptor-dependent pathway by which neutralization of low density lipoprotein receptor-related protein promotes fibrosarcoma cell migration and matrigel invasion. *J. Cell Sci.* **113**:123–134.
27. Ma, Z., et al. 2002. Regulation of Rac1 activation by the low density lipoprotein receptor-related protein. *J. Cell Biol.* **159**:1061–1070.
28. Zhu, Y., and Hui, D.Y. 2002. Low density lipoprotein receptor-related protein mediates apolipoprotein E inhibition of smooth muscle cell migration. *J. Biol. Chem.* **277**:4141–4146.
29. Boucher, P., Gotthardt, M., Li, W.P., Anderson, R.G., and Herz, J. 2003. LRP: role in vascular wall integrity and protection from atherosclerosis. *Science.* **300**:329–332.
30. Swertfeger, D.K., Bu, G., and Hui, D.Y. 2003. Apolipoprotein E binding to low density lipoprotein receptor-related protein-1 inhibits cell migration via activation of cAMP-dependent protein kinase A. *J. Biol. Chem.* **278**:36257–36263.
31. Orr, A.W., Elzie, C.A., Kucik, D.F., and Murphy-Ullrich, J.E. 2003. Thrombospondin signaling through the calreticulin/LDL receptor-related protein co-complex stimulates random and directed cell migration. *J. Cell. Sci.* **116**:2917–2927.
32. Tanaga, K., et al. 2004. LRP1B attenuates the migration of smooth muscle cells by reducing membrane localization of urokinase and PDGF receptors. *Arterioscler. Thromb. Vasc. Biol.* **24**:1422–1428.
33. Seki, N., et al. 2005. LRP1B is a negative modulator of increased migration activity of intimal smooth muscle cells from rabbit aortic plaques. *Biochem. Biophys. Res. Commun.* **331**:964–970.
34. Nykjaer, A., et al. 1997. Recycling of the urokinase receptor upon internalization of the uPA:serpin complexes. *EMBO J.* **16**:2610–2620.
35. Liu, C.X., et al. 2001. The putative tumor suppressor LRP1B, a novel member of the low density lipoprotein (LDL) receptor family, exhibits both overlapping and distinct properties with the LDL receptor-related protein. *J. Biol. Chem.* **276**:28889–28896.
36. Degryse, B., et al. 2001. Urokinase/urokinase receptor and vitronectin/alpha(v)beta(3) integrin induce chemotaxis and cytoskeleton reorganization through different signaling pathways. *Oncogene.* **20**:2032–2043.
37. Cohn, R.D., et al. 2007. Angiotensin II type 1 receptor blockade attenuates TGF-beta-induced failure of muscle regeneration in multiple myopathic states. *Nat. Med.* **13**:204–210.
38. Boucher, P., et al. 2007. LRP1 functions as an atheroprotective integrator of TGFbeta and PDGF signals in the vascular wall: implications for Marfan syndrome. *PLoS ONE.* **2**:e448.
39. Rogaeva, E., et al. 2007. The neuronal sortilin-related receptor SORL1 is genetically associated with Alzheimer disease. *Nat. Genet.* **39**:168–177.
40. Scherzer, C.R., et al. 2004. Loss of apolipoprotein E receptor LR11 in Alzheimer disease. *Arch. Neurol.* **61**:1200–1205.
41. Sagare, A., et al. 2007. Clearance of amyloid-beta by circulating lipoprotein receptors. *Nat. Med.* **13**:1029–1031.
42. Fujita, Y., et al. 2005. Association of nucleotide variations in the apolipoprotein B48 receptor gene (APOB48R) with hypercholesterolemia. *J. Hum. Genet.* **50**:203–209.
43. Taira, K., et al. 2002. Positive family history for coronary heart disease and 'midband lipoproteins' are potential risk factors of carotid atherosclerosis in familial hypercholesterolemia. *Atherosclerosis.* **160**:391–397.
44. Bujo, H., et al. 1994. Chicken oocyte growth is mediated by an eight ligand binding repeat member of the LDL receptor family. *EMBO J.* **13**:5163–5175.
45. Kobayashi, K., et al. 2005. Targeted disruption of TGF-beta-Smad3 signaling leads to enhanced neointimal hyperplasia with diminished matrix deposition in response to vascular injury. *Circ. Res.* **96**:904–912.
46. Hirata, T., Unoki, H., Bujo, H., Ueno, K., and Saito, Y. 2006. Activation of diacylglycerol O-acyltransferase 1 gene results in increased tumor necrosis factor-alpha gene expression in 3T3-L1 adipocytes. *FEBS Lett.* **580**:5117–5121.
47. Bujo, H., et al. 1995. Mutant oocytic low density lipoprotein receptor gene family member causes atherosclerosis and female sterility. *Proc. Natl. Acad. Sci. U. S. A.* **92**:9905–9909.
48. Redmond, E.M., et al. 2001. Endothelial cells inhibit flow-induced smooth muscle cell migration: role of plasminogen activator inhibitor-1. *Circulation.* **103**:597–603.

Matrix Metalloproteinase-3 Enhances the Free Fatty Acids-Induced VEGF Expression in Adipocytes Through Toll-Like Receptor 2

TORU KAWAMURA,* KENTARO MURAKAMI,* HIDEAKI BUJO,†,[1] HIROYUKI UNOKI,‡ MEIZI JIANG,† TOSHINORI NAKAYAMA,§ AND YASUSHI SAITO*

*Department of Clinical Cell Biology, †Department of Genome Research and Clinical Application, ‡Department of Applied Translation Research, and §Department of Immunology, Chiba University Graduate School of Medicine, Chuo-ku, Chiba 260-8670, Japan

Infiltrated macrophages (Mϕ) are believed to cause pathological changes in the surrounding adipocytes through the secretion of active molecules in visceral fat. Matrix metalloproteinase (MMP)-3 is secreted from Mϕ, and enhances expression of the inflammatory cytokines through the activation of toll-like receptor (TLR) 2. Visceral adipocytes express high levels of vascular endothelial growth factor (VEGF), and the degree of visceral fat accumulation is associated with the plasma VEGF concentration in obese subjects. The aim of the study is to clarify the role of MMP-3 in the enhancement of the free fatty acids (FFAs)-induced VEGF expression through TLR2 in visceral adipocytes. One mM FFAs induced VEGF mRNA and protein expression in 3T3-L1 adipocytes. The FFAs-induced VEGF expression was mostly mediated by TLR2. A high fat intake increased the VEGF mRNA expression in visceral fat and the VEGF concentration in plasma, accompanied with the increase in the plasma FFAs concentration in mice. These increases were largely inhibited in TLR2-deficient mice. The FFAs-induced VEGF expression was increased in the presence of Mϕ-conditioned medium (CM) in adipocytes, and the enhancement was inhibited by a MMP-3 inhibitor or a neutralizing antibody against MMP-3. The active form of MMP-3 induced the VEGF mRNA expression, as well as TLR2, in adipocytes. The increase in the VEGF expression by MMP-3 was inhibited by the treatment with siRNA for TLR2. The enhancement of FFAs-induced TLR2 expression by Mϕ-CM was inhibited by blocking of the MMP-3. The increase in the VEGF mRNA expression by Mϕ-CM or MMP-3 was partially inhibited by a neutralizing antibody against TNF-α. These results indicate that MMP-3 in Mϕ-CM enhances the FFAs-induced VEGF expression in adipocytes through the increase in the TLR2 expression. The MMP-3 secreted from the infiltrated Mϕ may be a regulator of the VEGF expression in visceral adipocytes. Exp Biol Med 233:1213–1221, 2008

Key words: matrix metalloproteinase-3; toll-like receptor 2; macrophage; vascular endothelial growth factor; adipocyte; visceral fat

Introduction

Adipocytes secrete a wide variety of cytokines, and some cause metabolic disturbance through the development of insulin resistance (1–3). The expression of toll-like receptor (TLR) 2 gene is associated with the gene expression of TNF-α (4), one of the cytokines that causes an inhibition of insulin signals in fat, muscle and liver (1–3, 5). High fat feeding leads to an increased population of TLR2/TNF-α co-expressing adipocytes in visceral fat, but not in subcutaneous fat in mice (4). A microarray analysis revealed that the accumulated visceral fat is accompanied with drastic changes in expression of matrix metalloproteinase (MMP) family genes, among which MMP-3 potentiated free fatty acids (FFAs)-induced TNF-α secretion from adipocytes (6). Infiltrated macrophage (Mϕ) has a potential for a pathological link with surrounding adipocytes through the secretion of MMP-3 followed by TNF-α expression in adipocytes in visceral fat tissue (7).

Vascular endothelial growth factor (VEGF) is abundantly secreted from adipocytes, and it plays a key role in the process of fat tissue formation through the regulation of angiogenesis in the tissues (8). The inhibition of angiogenesis leads to a decreased volume of developing fat tissue or fat grafting after transplantation in mice (9, 10). VEGF is highly expressed in visceral fat, and the circulating VEGF concentration is positively correlated with visceral fat

This work was partly supported by Grants-in-Aid for Scientific Research to H.B. and Y.S. from the Ministry of Education, Culture, Sports, Science and Technology, Japan.

[1] To whom correspondence should be addressed at Department of Genome Research and Clinical Application, Chiba University Graduate School of Medicine, 1-8-1 Inohana, Chuo-ku, Chiba 260-8670, Japan. E-mail: hbujo@faculty.chiba-u.jp

Received January 18, 2008.
Accepted May 7, 2008.

DOI: 10.3181/0801-RM-20
1535-3702/08/23310-1213$15.00

volume in obese mice (11). These observations suggest that the TLR2 expression in adipocytes is related to the expression of VEGF as well as TNF-α. In this context, the tight association between visceral fat accumulation and the plasma VEGF level is in fact observed in obese human subjects (12). However, the mechanism for the induction of VEGF expression in visceral fat has not been elucidated.

FFAs have been shown to activate the downstream signals of TLR2 (13, 14). The aim of this study was to clarify the role of MMP-3 in the enhancement of the FFAs-induced VEGF expression through TLR2 in visceral adipocytes. The significance of TLR2 for the FFAs-induced VEGF expression was at first analyzed in cultured adipocytes and the visceral fat of TLR2-deficient mice. Next, the possible pathological role of the MMP-3 secreted from Mϕ in the FFAs-induced VEGF expression through TLR2 was assessed in a culture system using conditioned medium (CM) of Mϕ.

Materials and Methods

Adipocyte Culture. 3T3-L1 preadipocytes (American Type Culture Collection, Rockville, MD) were cultured in high-glucose DMEM (DMEM-H, GibcoBRL, Tokyo, Japan) supplemented with 10% FBS (Sigma, St. Louis, MO) and antibiotics. After the 3T3-L1 preadipocytes were grown to near confluence, the differentiation to mature adipocytes was performed using insulin (Sigma), dexamethasone (Sigma), and 3-isobutyl-1-methyl-xanthine (Sigma), as described previously (7). A vast majority of cells (~90%) had accumulated lipid droplets between 10–14 days after differentiation and were used for further experiments.

Cell Treatment with FFAs. The treatment of 3T3-L1 cells with FFAs was performed essentially according to the method previously described (15). After overnight incubation in serum-free DMEM-H supplemented with 0.1% FFAs-free BSA, the cells were treated in serum-free DMEM-H supplemented with 0.1% FFAs-free BSA with 1 mM FFAs (a cocktail containing 0.5 mM palmitic acid and 0.5 mM myristic acid, Sigma) for indicated times, and then incubated in serum-free DMEM-H supplemented with 0.1% FFAs-free BSA with 1 mM FFAs in the presence or absence of 1 μg/ml zymosan A (Wako, Tokyo, Japan), 10 μg/ml peptidoglycan (PGN, Invitrogen, Tokyo, Japan), or 100 μg/ml active form of MMP-3 purified from human fibroblasts (Sigma), a neutralizing antibody against TNF-α (15) (R&D Systems, Minneapolis, MN) or non-immune IgG (R&D Systems) for indicated times. The composition ratio of FFAs/BSA in the medium corresponds to 6:1 for the first incubation medium.

Quantitative Real-Time Reverse Transcriptase-Polymerase Chain Relation (RT-PCR). Total RNA was extracted from fat tissue or 3T3-L1 adipocytes using RNeasy Mini kit (QIAGEN, Valencia, CA), and was reverse transcribed using the GeneAmp Gold RNA PCR Reagent kit (PE Applied Biosystems, Foster City, CA) as described previously (7). Quantitative RT-PCR amplifications were performed using TaqMan Universal PCR Master Mix and Assay-on-Demand Gene expression Assay Mix specific for mouse VEGF A (Mm00437304_m1) or TLR2 (Mm00442346_m1) mRNA. All PCRs were performed in an ABI PRISM 7500 sequence detection system (PE Applied Biosystems).

Enzyme-Linked Immunosorbent Assay (ELISA). The VEGF concentration of plasma or cell culture medium was measured using a Quantikine Mouse VEGF Immunoassay kit (R&D Systems).

siRNA Knockdown Treatment. 3T3-L1 adipocytes or THP-1-derived Mϕ were transfected either with 5 nmol siRNA for TLR2 (QIAGEN) or MMP-3 (Invitrogen), or Allstars Negative Control (QIAGEN) siRNA by electroporation as described previously (7). The cells were reseeded after electroporation, and incubated with DMEM-H containing 10% FBS for two days. After overnight incubation in serum-free DMEM-H supplemented with 0.1% FFA-free BSA, the siRNA-treated 3T3-L1 adipocytes were incubated in serum-free DMEM-H supplemented with 0.1% FFA-free BSA and 1 mM FFAs for 6 h. The CM of the siRNA-treated Mϕ was prepared by the incubation for the following 24 h.

Mice. $TLR2^{-/-}$ mice were kindly provided by Dr. Shizuo Akira (Osaka University) (16). Briefly, mouse TLR2 gene was disrupted by introducing a targeted mutation into E14.1 embryonic stem cells. A targeting vector was designed to replace a part of the exon that encodes the transmembrane and the cytoplasmic domain of TLR2 with the *neo* gene. ES cell lines containing a mutant TLR2 allele were microinjected into C57BL/6 blastocysts. Heterozygous mice were intercrossed to produce $TLR2^{-/-}$ mice and $TLR2^{+/+}$ mice. The $TLR2^{-/-}$ mice grew healthy and did not show any obvious abnormality until 20 weeks. TLR2 mRNA could not be detected in either the mesenteric or subcutaneous fat tissue of the $TLR2^{-/-}$ mice. From five weeks of age, female $TLR2^{+/+}$ and $TLR2^{-/-}$ mice were given either a regular (D12450B, Research Diet, New Brunswick, NJ, see Table 1) or a high fat diet (D12492).

Preparation of Mϕ-CM. The preparation of Mϕ-CM was performed essentially as described (7). The human monocytic cell line THP-1 (American Type Culture Collection) was cultured in RPMI 1640 supplemented with l-glutamine (GibcoBRL) and antibiotics and 10% FBS. To allow the monocytes to differentiate into adherent macrophages, THP-1 cells were washed in PBS (calcium- and magnesium-free, GibcoBRL, medium A) and re-suspended in fresh medium A containing 50 ng/ml phorbol 12-myristate–13-acetate (PMA, Sigma) for 3 days (at day 0). The cells were incubated for 3 more days in DMEM supplemented with 2% BSA, and then at day 4, the cells were treated for the CM preparation for 24 h. Control CM was prepared by incubating the THP-1 cells without the differentiation treatment (THP1-CM).

Treatment of Adipocytes with Mϕ-CM. After treatment in serum-free DMEM-H supplemented with

Table 1. Contents of Regular and High Fat Diets

	Regular diet (D12450B)		High fat diet (D12492)	
	g %	kcal %	g %	kcal %
Protein	19.2	20	26.2	20
Carbohydrate	67.3	70	26.3	20
Fat	4.3	10	34.9	60
Total		100		100
kcal/g	3.85		5.24	
	g	kcal	g	kcal
Casein, 80 mesh	200	800	200	800
L-Cystine	3	12	3	12
Corn starch	315	1260	0	0
Maltodextrin 10	35	140	125	500
Sucrose	350	1400	68.8	275.2
Cellulose, BW200	50	0	50	0
Soybean oil	25	225	25	225
Lard	20	180	245	2205
Mineral mix S10026	10	0	10	0
DiCalcium phosphate	13	0	13	0
Calcium carbonate	5.5	0	5.5	0
Potassium citrate, 1 H2O	16.5	0	16.5	0
Vitamin mix V10001	10	40	10	40
Choline bitartrate	2	0	2	0
Total	1055.05	4057	773.85	4075

0.1% FFA-free BSA and 1 mM FFAs for 6 h, 3T3-L1 adipocytes were incubated in serum-free DMEM-H supplemented with 0.1% FFA-free BSA and 1 mM FFAs with Mϕ-CM or THP1-CM at 10% of the final volume, or the active form of MMP-3 for the indicated time periods. Mϕ-CM or THP1-CM was treated with an MMP-3 inhibitor, NNGH (*N*-isobutyl-*N*-(4-methoxyphenylsulfonyl)-glycyl-hydroxamic acid; Calbiochem, San Diego, CA) (17, 18), goat anti-MMP-3 polyclonal antibody (Santa Cruz, Santa Cruz, CA) or non-immune goat IgG (Santa Cruz) for 12 h, prior to the addition to adipocytes.

Statistical Analyses. The results are presented as the mean ± SD. Statistical significance between two groups was evaluated by Student's *t*-test. Statistical significance among several groups was performed using a one-way ANOVA. A value of $P < 0.05$ was considered to be significant.

Results

FFAs-Induced VEGF mRNA Expression Is Mediated by TLR2 in 3T3-L1 Adipocytes. FFAs induce the TNF-α expression through the increased TLR2 expression in adipocytes (4). The effect of FFAs on the expression of VEGF mRNA through TLR2 was analyzed in 3T3-L1 adipocytes. The VEGF mRNA expression levels were increased time-dependently in the presence of 1 mM FFAs (a cocktail containing 0.5 mM palmitic acid and 0.5 mM myristic acid) (Fig. 1A). The VEGF concentration in the medium for 72 hr after incubation of 3T3-L1 adipocytes in the presence of 1 mM FFAs was significantly higher than that in the absence of FFAs (Fig. 1B). Zymosan A, a TLR2 ligand that induces the TNF-α mRNA expression in 3T3-L1 adipocytes (4, 19), showed the effect additive to the treatment with FFAs on the increase in the VEGF mRNA expression in the cells (Fig. 1C). Furthermore, the VEGF mRNA expression was increased to 1.8-fold by 10 g/ml peptidoglycan (PGN), another TLR2 ligand (19), in comparison to that without the addition in the cells incubated with FFAs (data not shown). The FFAs-induced increase in the VEGF mRNA expression level was mostly abolished in the adipocytes transfected with TLR2-specific siRNA in comparison to that in the cells transfected with control siRNA (Fig. 1D). These results indicate that FFAs-induced VEGF mRNA expression is most likely mediated by TLR2 in 3T3-L1 adipocytes.

A High Fat Intake Increases the VEGF mRNA Expression in Visceral Fat, Accompanied with an Increase in Plasma VEGF Concentration in TLR2$^{+/+}$ Mice, but Not in TLR2$^{-/-}$ Mice. The above observations for the FFAs-induced VEGF expression through TLR2 in cultured adipocytes suggest that a high fat intake may induce the VEGF mRNA expression through the FFAs-mediated TLR2 expression in fat tissues. The expression levels of VEGF mRNA in the fat tissues of TLR2$^{+/+}$ mice and TLR2$^{-/-}$ mice were invcstigated after fat feeding for six weeks. Plasma FFAs levels were significantly increased in the high fat-fed TLR2$^{+/+}$ mice in comparison to those in the regular diet-fed TLR2$^{+/+}$ mice, and were not significantly different from the high fat-fed TLR2$^{-/-}$ mice (Fig. 2A). The expression levels of VEGF mRNA in mesenteric fat were significantly increased in the high fat-fed TLR2$^{+/+}$ mice in comparison to those in regular

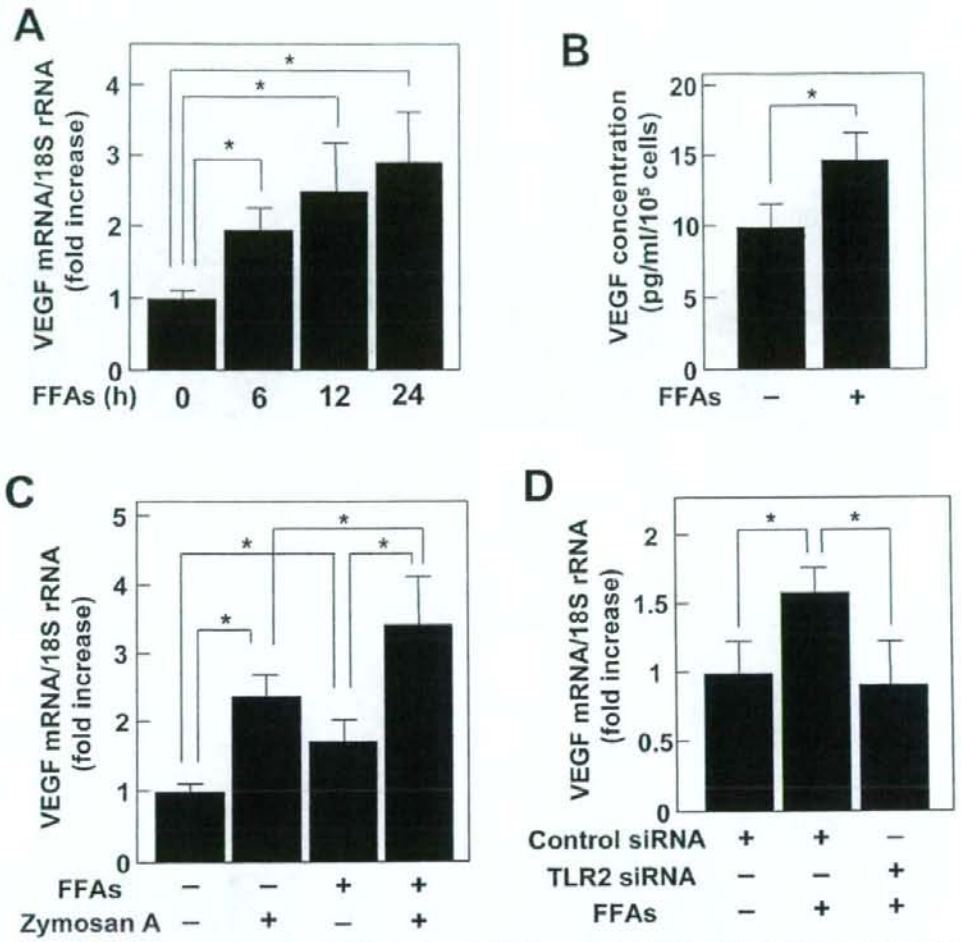

Figure 1. The effect of FFAs with zymosan A or TLR2 knockdown on the VEGF expression in 3T3-L1 adipocytes. (A) Total RNA was extracted from adipocytes after incubation with 1 mM FFAs (a cocktail of 0.5 mM palmitic acid and 0.5 mM myristic acid) for indicated time. The VEGF mRNA level was evaluated by quantitative real-time RT-PCR. mRNA levels were calculated as the fold increase of the control at 0 h. The bars represent the mean ± SD ($n = 3$). * $P < 0.05$. (B) Conditioned media were collected after incubation of adipocytes with 1 mM FFAs for 72 h. The VEGF concentration was measured using ELISA, and then presented by the correction with the incubated cell number. The cell appearance was not changed after the incubation with FFAs, and no significant difference was observed in the cell counts between the adipocytes incubated with and without FFAs. The bars represent the mean ± SD ($n = 3$). * $P < 0.05$. (C) Adipocytes were incubated with or without 1 mM FFAs for 6 h, and then with or without 1 mM FFAs in the presence or absence of 1 μg/ml Zymosan A for 6 h. Total RNA was extracted from adipocytes, and the VEGF mRNA level was evaluated by quantitative real-time RT-PCR. The mRNA levels were calculated as the fold increase of the control in the absence of FFAs or zymosan A. The bars represent the mean ± SD ($n = 3$). * $P < 0.05$. (D) Adipocytes were transfected either with TLR2-specific siRNA or control siRNA. Total RNA was extracted from the adipocytes after incubation with or without 1 mM FFA for 6 h. The mRNA levels were calculated as the fold increase of those of cells transfected with control siRNA without the FFA treatment. The bars represent the mean ± SD ($n = 5$). * $P < 0.05$.

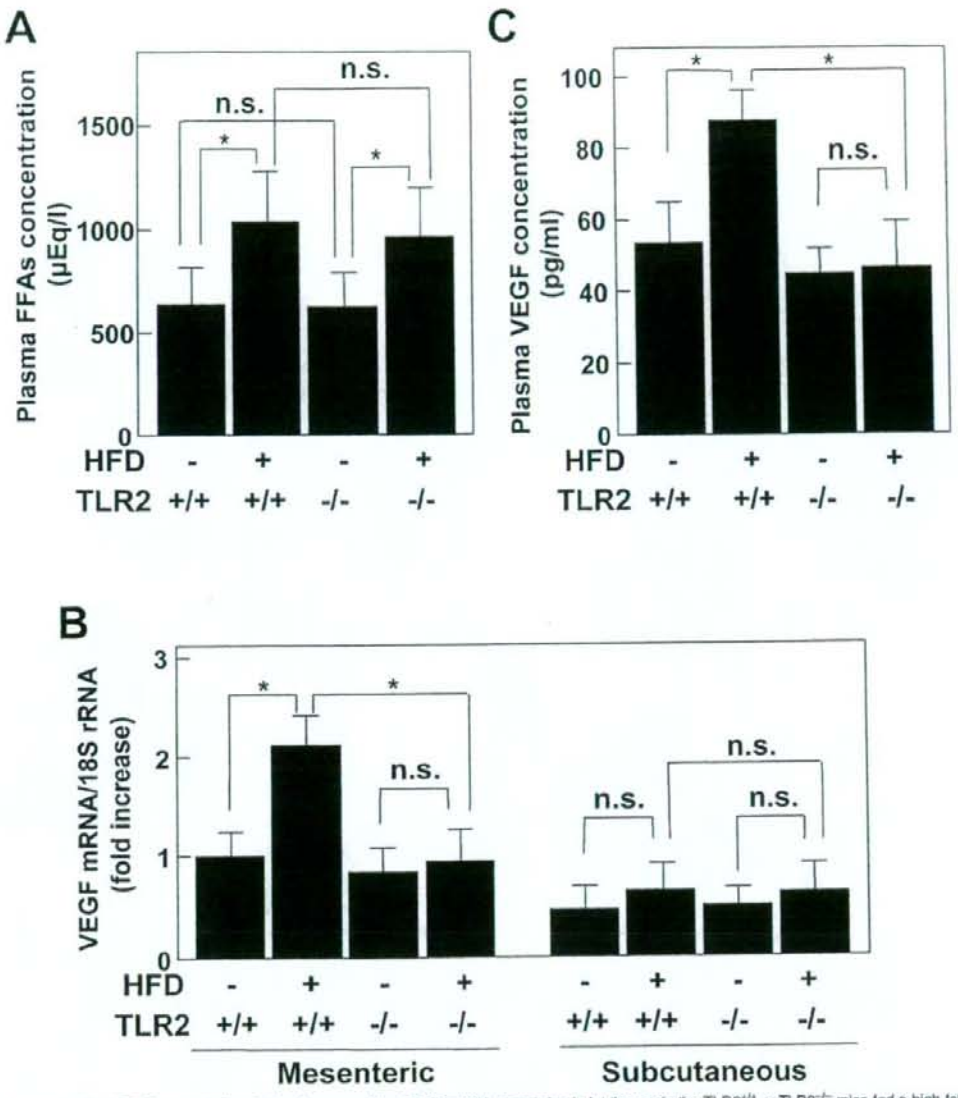

Figure 2. The VEGF concentration in the plasma and the VEGF mRNA expression in fat tissues in the $TLR2^{+/+}$ or $TLR2^{-/-}$ mice fed a high fat diet (HFD) for four weeks. (A) The plasma FFAs concentrations in $TLR2^{-/-}$ and $TLR2^{-/-}$ mice with or without a HFD diet. The bars represent the mean ± SD ($n = 5$). * $P < 0.05$. (B) Total RNA was extracted from either mesenteric or subcutaneous fat tissue specimens of mice. The mRNA levels corrected by protein weight of tissues were calculated as the fold increase of the control in mesenteric fat of $TLR2^{-/-}$ mice without a HFD feeding (note: the fold increases of the control for 3T3-L1 preadipocyte and adipocyte are 0.17 ± 0.04 and 0.59 ± 0.18, respectively). The bars represent the mean ± SD ($n = 5$). * $P < 0.05$. n.s., not significant. (C) The plasma VEGF concentration was measured using an ELISA. The bars represent the mean ± SD ($n = 5$). * $P < 0.05$.

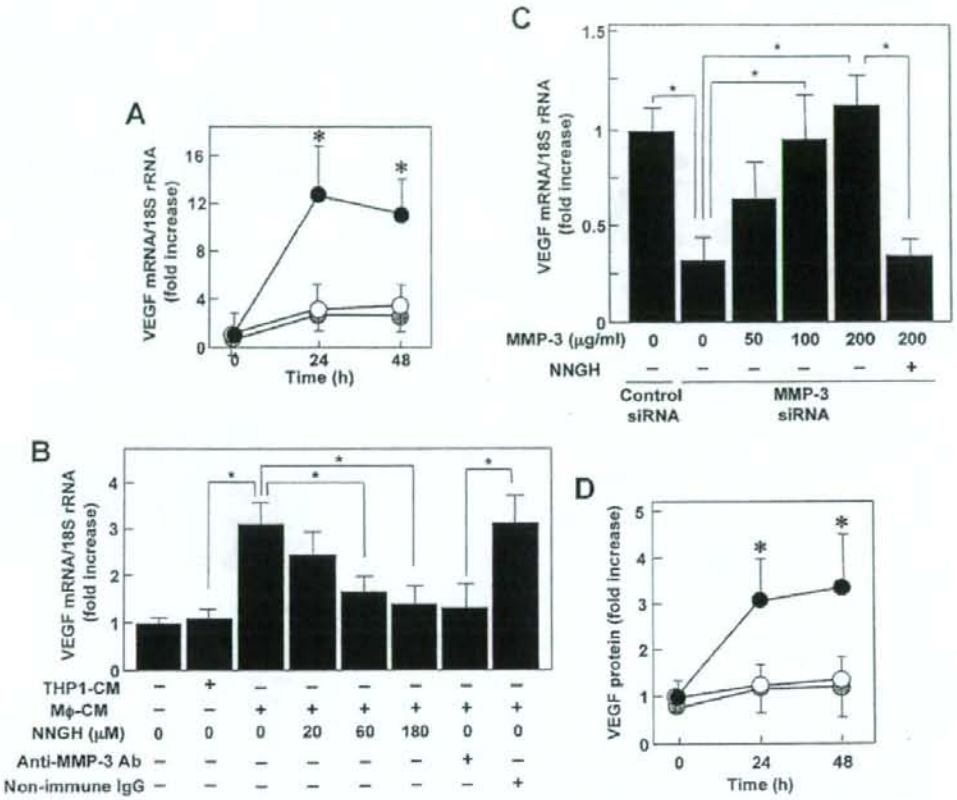

Figure 3. Effect of MMP-3 blocking on the FFAs-induced VEGF expression enhanced by Mϕ-CM in 3T3-L1 adipocytes. (A) 3T3-L1 adipocytes were incubated with (open and closed circles) or without (gray circle) 1 mM FFAs in the presence of 10% THP1-CM (open circle) or 10% Mϕ-CM (closed and gray circles) for indicated time in the presence (open and closed circles) or absence (gray circle) of preincubation with 1 mM FFAs for 6 h. Total RNA was extracted from adipocytes, and the VEGF mRNA level was evaluated by quantitative real-time RT-PCR. mRNA levels were calculated as the fold increase of control at 0 h in the absence of CM after the treatment with FFAs. The bars represent the mean ± SD (n= 3). * $P < 0.05$ vs. cells in the absence of CM after the treatment with FFAs. (B) After the incubation with 1 mM FFAs for 6 h, 3T3-L1 adipocytes were treated with or without 10% THP1-CM, 10% Mϕ-CM, 20–180 μM NNGH, anti-MMP-3 neutralizing antibody, or non-immune IgG, in the presence of 1 mM FFAs for 6 h. Total RNA was extracted from adipocytes, and the VEGF mRNA level was evaluated by quantitative real-time RT-PCR. mRNA levels were calculated as the fold increase of control in the absence of CM, NNGH or antibody. The bars represent the mean ± SD (n = 3). * $P < 0.05$. (C) 3T3-L1 adipocytes were transfected either with MMP-3-specific or control siRNA. Total RNA was extracted from adipocytes incubated with or without 50–200 μg/ml MMP-3 or 60 μM NNGH in the presence of 1mM FFAs for 6 h after pre-incubation with 1 mM FFAs for 6 h. Total RNA was extracted from adipocytes, and the VEGF mRNA level was evaluated by quantitative real-time RT-PCR. The mRNA levels were calculated as the fold increase of that in cells transfected with control siRNA in the absence of MMP-3 and NNGH. The bars represent the mean ± SD (n=3). * $P < 0.05$. (D) 3T3-L1 adipocytes were incubated with (open and closed circles) or without (gray circle) 1 mM FFAs in the presence of 10% THP1-CM (open circle) or 10% Mϕ-CM (closed and gray circles) for indicated time in the presence (open and closed circles) or absence (gray circle) of pre-incubation with 1 mM FFAs for 6 h. The incubated media were collected, and the VEGF concentration was measured using ELISA. The concentration levels were calculated as the fold increase of control at 0 h in the absence of CM after the treatment with FFAs. The bars represent the mean ± SD (n = 3). * $P < 0.05$ vs. cells in the absence of CM after the treatment with FFAs. * $P < 0.05$.

diet-fed TLR2$^{+/+}$ mice (Fig. 2B). However, the expression levels of VEGF mRNA in the mesenteric fat did not significantly change between the TLR2$^{-/-}$ mice fed a regular diet and a high fat diet. Thus, the increase in the expression levels of VEGF mRNA in the mesenteric fat of the high fat-fed TLR2$^{+/+}$ mice were not observed in high fat-fed TLR2$^{-/-}$ mice. There were no significant differences in the VEGF mRNA expression levels in the subcutaneous fat either between the high fat-fed TLR2$^{+/+}$ mice and the regular diet-fed TLR2$^{+/+}$ mice, or between the high fat-fed

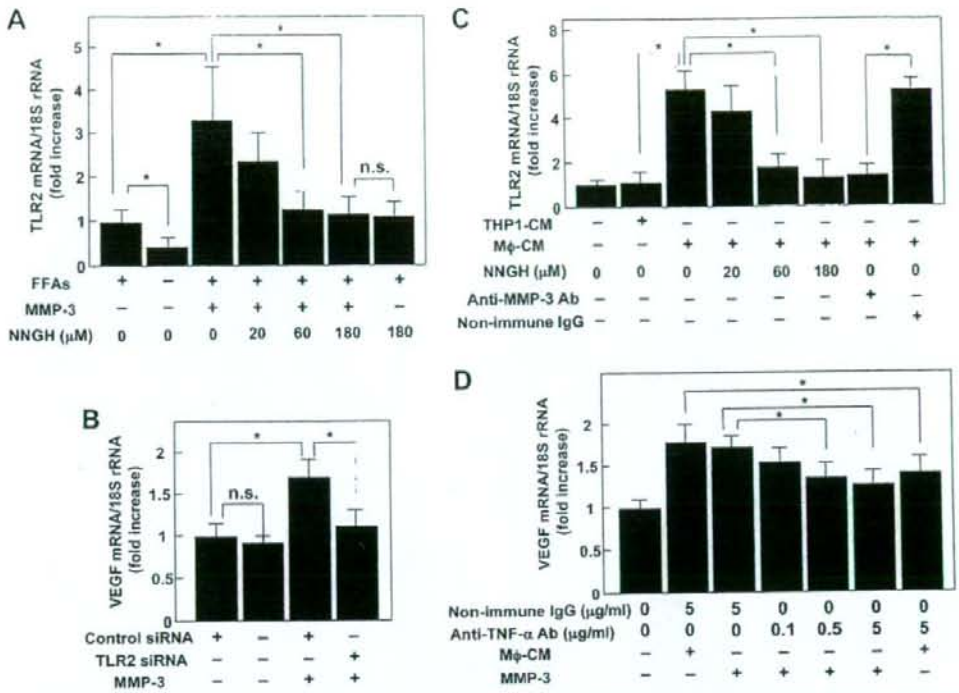

Figure 4. Effect of MMP-3 on the FFAs-induced TLR2 and VEGF expression in 3T3-L1 adipocytes. (A) After the incubation with 1 mM FFAs for 6 h, adipocytes were treated with or without the active form of MMP-3 (100 μg/ml) or 20–180 μM NNGH in the presence of 1 mM FFAs for 6 h. Total RNA was extracted from adipocytes, and the VEGF mRNA level was evaluated by quantitative real-time RT-PCR. mRNA levels were calculated as the fold increase of control without MMP-3 or NNGH. The bars represent the mean ± SD ($n=3$). * $P<0.05$. (B) Adipocytes were transfected either with TLR2-specific siRNA or control siRNA. After the incubation with 1 mM FFAs for 6 h, cells were treated with or without MMP-3 (100 μg/ml) in the presence of 1 mM FFAs for 6 h. Total RNA was extracted from adipocytes, and the mRNA levels were calculated as a fold increase of control in cells transfected with control siRNA without MMP-3. The bars represent the mean ± SD ($n=4$). * $P<0.05$. (C) After the incubation with 1 mM FFAs for 6 h, adipocytes were treated with or without 10% THP1-CM, 10% Mϕ-CM, 20–180 μM NNGH, anti-MMP-3 neutralizing antibody, or non-immune IgG in the presence of 1 mM FFAs for 6 h. Total RNA was extracted from adipocytes, and the TLR2 mRNA level was evaluated by quantitative real-time RT-PCR. mRNA levels were calculated as the fold increase of the control in the absence of CM or NNGH. The bars represent the mean ± SD ($n=4$). * $P<0.05$. (D) After the incubation with 1 mM FFAs for 6 h, adipocytes were treated with or without 10% Mϕ-CM, 100 μg/ml MMP-3, 0.5–5 μg/ml anti-TNF-α neutralizing antibody or 5 μg/ml non-immune IgG for 24 h in the presence of 1 mM FFAs for 6 h. Total RNA was extracted from adipocytes, and the VEGF mRNA level was evaluated by quantitative real-time RT-PCR. mRNA levels were calculated as the fold increase of the control in the absence of antibody, CM or MMP-3. The bars represent the mean ± SD ($n=4$). * $P<0.05$.

$TLR2^{+/+}$ mice and the high fat-fed $TLR2^{-/-}$ mice. The plasma VEGF concentration was significantly increased in the high fat-fed $TLR2^{+/+}$ mice in comparison to those in the regular diet-fed $TLR2^{+/+}$ mice (Fig. 2C). The plasma VEGF level in the high fat-fed $TLR2^{-/-}$ mice did not change in comparison to that in the regular diet-fed $TLR2^{-/-}$ mice, and significantly decreased in comparison to those of the high fat-fed $TLR2^{+/+}$ mice. Thus, the TLR2 ablation abolished an increase in the VEGF mRNA expression in the visceral fat and the plasma VEGF concentration in the mice fed a high fat diet.

Mϕ Enhances the FFAs-Induced VEGF mRNA Expression in Adipocytes Through MMP-3. Infiltrated Mϕ causes the induction of TNF-α expression in the adipocytes of visceral fat tissues (20, 21). A recent study identified that MMP-3 is secreted from Mϕ, and responsible for the induction for the TNF-α expression using co-culture system (7). To assess whether MMP-3 is a regulatory player for the VEGF expression in adipocytes accumulated in mesenteric regions, the blocking effect of MMP-3 on the action of Mϕ-CM for the FFAs-induced VEGF mRNA expression was firstly examined in 3T3-L1 adipocytes. The addition of Mϕ-CM significantly enhanced the VEGF mRNA expression in the adipocytes treated with 1 mM FFAs for 6 h, but not in cells without the treatment with FFAs (Fig. 3A). The stimulatory effect of Mϕ-CM on the FFAs-induced VEGF mRNA expression was dose-dependently inhibited by the treatment of adipocytes with NNGH, a

specific inhibitor of MMP-3 (17), in the range similar to that for the inhibition of MMP-3 in microglia (18) (Fig. 3B). The effect of Mϕ-CM on the FFAs–induced VEGF mRNA expression was also inhibited by the treatment of an anti-MMP-3 neutralizing antibody to an extent similar to that by NNGH. In addition, the stimulatory effect of Mϕ-CM on the FFAs-induced VEGF mRNA expression was not observed using the CM of Mϕ pretreated with siRNA specific for MMP3 (Fig. 3C), and the decreased VEGF mRNA expression increased by the addition of active form of MMP-3 in a dose-dependent manner; the recovered expression level by the addition of 200 μg/ml MMP-3 was again inhibited to that without MMP-3 by the incubation together with NNGH at 60 μM. Finally, the VEGF concentration in the media of 3T3-L1 adipocytes significantly increased in the presence of active form of MMP-3 in addition to the treatment with 1 mM FFAs, in comparison to those in the absence of MMP-3 or without the incubation with FFA (Fig. 3D). These results strongly suggest that Mϕ enhances the FFAs-induced VEGF mRNA expression in adipocytes, in part through the action of secreted MMP-3.

MMP-3, Secreted from Mϕ, Enhances the FFAs-Induced VEGF Expression Through the Expression and Activation of TLR2 in Adipocytes. We have shown that the expression of TLR2 is tightly associated with that of TNF-α in visceral adipocytes, and the population of TLR2/TNF-α co-expressing adipocytes is increased in visceral fat of the high fat-fed mice (4). Therefore, the role of TLR2 in the enhancement of FFAs-induced VEGF mRNA expression by MMP3 was analyzed in 3T3-L1 adipocytes. The TLR2 mRNA expression level after treatment with 1mM FFAs for 6 h was significantly increased by the incubation of adipocytes with active form of MMP-3 (Fig. 4A). The increase in the expression level of TLR2 mRNA in the presence of MMP-3 was dose-dependently inhibited by the treatment together with NNGH. Furthermore, the VEGF mRNA expression induced by MMP-3 was abolished in the 3T3-L1 adipocytes treated with siRNA specific for TLR2 (Fig. 4B). The FFAs-induced TLR2 expression level was significantly increased in the presence of Mϕ-CM in comparison to that in the presence of THP-1-CM (Fig. 4C), and the increase in the FFAs-induced TLR2 expression level by the incubation with Mϕ-CM was decreased by the addition of NNGH or a neutralizing antibody against MMP-3; the dose range of NNGH for the inhibition of Mϕ-CM-mediated TLR2 expression was nearly the same as those for the Mϕ-CM-mediated VEGF mRNA expression and MMP-3-mediated TLR2 expression (Fig. 3B and 4A, respectively). Finally, we evaluated the effect of an addition of a neutralizing antibody against TNF-α in Mϕ-CM on the FFAs-induced VEGF mRNA expression at around 2 μg/ml, which is a concentration that was previously shown to block the TNF-α action in 3T3-L1 adipocytes (15) (Fig. 4D). The enhancement in the FFAs-induced VEGF mRNA expression by Mϕ-CM or MMP-3 was partially, but significantly, inhibited by the blocking of TNF-α. These results indicate that Mϕ, through the action of secreted MMP-3, enhances the FFAs-induced VEGF expression through the TLR2 expression, and in part the following expression of TNF-α in adipocytes.

Discussion

In the series of experiments using a culture system and TLR2-knockout mice, we at first investigated the role of TLR2 in the FFAs-induced VEGF expression in adipocytes. FFAs induced the VEGF mRNA and protein expressions, and the FFAs-induced VEGF expression was mostly mediated by TLR2. Next, a high fat intake caused significant increases in the VEGF mRNA expression in visceral fat and the VEGF concentration in plasma in mice, and the effects of a high fat intake were inhibited in TLR2-deficient mice. The FFAs-induced VEGF expression was increased in the presence of Mϕ-CM in 3T3-L1 adipocytes. The increased expression was almost inhibited by the blocking of MMP-3. Furthermore, active form of MMP-3 enhanced the FFAs-induced VEGF and TLR2 mRNA expression, and the increased VEGF expression by MMP-3 was not observed by the TLR2 knockdown in adipocytes. The enhancement of FFAs-induced TLR2 expression by Mϕ-CM was again almost completely inhibited by the blocking of MMP-3. Finally, the MMP-3-mediated VEGF expression was in part inhibited by the blocking of TNF-α in 3T3-L1 adipocytes. These results indicated that MMP-3, secreted from Mϕ, enhances the FFAs-induced VEGF expression through the induction in the expression of TLR2 and its downstream molecule, TNF-α, in adipocytes.

Adipocytes transplanted to the mesenteric regions express a variety of genes in comparison to those in the subcutaneous regions in mice (6). MMP-3 is one of the highly expressed genes in mesenteric regions, and enhanced the FFA-induced TNF-α secretion from adipocytes (7). The Mϕ infiltration has been observed in the accumulated fat tissues, and active Mϕ causes a change in the surrounding adipocytes in visceral fat, thus leading to the progression of insulin resistance (20, 21). The degree of visceral fat accumulation has shown to be closely associated with the development of insulin resistance (1, 2). A variety of inflammatory bioactive molecules play an important role in the pathological interaction between Mϕ and adipocytes in visceral fat (1–3, 20, 21). In this context, infiltrated Mϕ may thus have a pathological link with the surrounding adipocytes through the secretion of MMP-3 followed by the TLR2 and TNF-α expression in the adipocytes in visceral fat tissues.

The plasma VEGF concentration, as well as the VEGF gene expression in visceral fat, is induced in db/db and KK-Ay mice (11). A high fat intake causes an increase in the number of TLR2/TNF-α co-expressing adipocytes in visceral fat, but not in subcutaneous fat, in mice (4). The current study showed that TLR2 enhances the FFAs-

induced VEGF expression, as well as the TNF-α expression. The ablation of TLR2 expression reduced the FFAs-induced VEGF expression in cultured cells and plasma VEGF levels in high fat-fed mice. The mechanism of VEGF mRNA expression in TLR2-expressing adipocytes has not yet been fully elucidated. A recent study showed that the inflammatory cytokines, IL-6 and oncostatin M, up-regulate VEGF expression in fat tissues via the JAK/STAT pathways, and these effects were reflected by the increased visceral obesity accompanied with the increased plasma VEGF concentration in mice (22, 23). Hypoxia is another potent stimulus for VEGF mRNA expression in human adipocytes (24). There is a possibility that MMP-3 cleaves a protein in the Mϕ-CM that becomes a ligand for the TLR2 receptor or another receptor for the induction of TLR2 expression, in addition to the direct interaction of MMP-3 with the cell surface of adipocytes, in the present culture system. Further analyses to address the regulation of TLR2 expression by MMP-3 are thus called for to elucidate the specific VEGF expression in adipocytes of visceral fat and the relationships between the plasma VEGF concentration and visceral adiposity, which is tightly associated with the development of the insulin resistance associated.

1. Garg A. Regional adiposity and insulin resistance. J Clin Endocrinol Metab 89:4206–4210, 2004.
2. Matsuzawa Y. The metabolic syndrome and adipocytokines. FEBS Lett 580:2917–2921, 2006.
3. Pittas AG, Joseph NA, Greenberg AS. Adipocytokines and insulin resistance. J Clin Endocrinol Metab 89:447–452, 2004.
4. Murakami K, Bujo H, Unoki H, Saito Y. High fat intake induces a population of adipocytes to co-express TLR2 and TNFalpha in mice with insulin resistance. Biochem Biophys Res Commun 354:727–734, 2007.
5. Hotamisligil GS, Arner P, Caro JF, Atkinson RL, Spiegelman BM. Increased adipose tissue expression of tumor necrosis factor-alpha in human obesity and insulin resistance. J Clin Invest 95:2409–2415, 1995.
6. Unoki H, Bujo H, Shibasaki M, Saito Y. Increased matrix metalloproteinase-3 mRNA expression in visceral fat in mice implanted with cultured preadipocytes. Biochem Biophys Res Commun 350:392–398, 2006.
7. Unoki H, Bujo H, Jiang M, Kawamura T, Murakami K, Saito Y. Macrophages regulate tumor necrosis factor-α expression in adipocytes through the secretion of matrix metalloproteinase-3. Int J Obesity 32: 902–915.
8. Voros G, Maquoi E, Demeulemeester D, Clerx N, Collen D, Lijnen HR. Modulation of angiogenesis during adipose tissue development in murine models of obesity. Endocrinology 146:4545–4554, 2005.
9. Yamaguchi M, Matsumoto F, Bujo H, Shibasaki M, Takahashi K, Yoshimoto S, Ichinose M, Saito Y. Revascularization determines volume retention and gene expression by fat grafts in mice. Exp Biol Med (Maywood) 230:742–748, 2005.
10. Rupnick MA, Panigrahy D, Zhang CY, Dallabrida SM, Lowell BB, Langer R, Folkman MJ. Adipose tissue mass can be regulated through the vasculature. Proc Natl Acad Sci U S A 99:10730–10735, 2002.
11. Miyazawa-Hoshimoto S, Takahashi K, Bujo H, Hashimoto N, Yagui K, Saito Y. Roles of degree of fat deposition and its localization on VEGF expression in adipocytes. Am J Physiol Endocrinol Metab 288:E1128–E1136, 2005.
12. Miyazawa-Hoshimoto S, Takahashi K, Bujo H, Hashimoto N, Saito Y. Elevated serum vascular endothelial growth factor is associated with visceral fat accumulation in human obese subjects. Diabetologia 46: 1483–1488, 2003.
13. Lee JY, Zhao L, Youn HS, Weatherill AR, Tapping R, Feng L, Lee WH, Fitzgerald KA, Hwang DH. Saturated fatty acid activates but polyunsaturated fatty acid inhibits toll-like receptor 2 dimerized with toll-like receptor 6 or 1. J Biol Chem 279:16971–16979, 2004.
14. Nguyen MT, Favelyukis S, Nguyen AK, Reichart D, Scott PA, Jenn A, Liu-Bryan R, Glass CK, Neels JG, Olefsky JM. A subpopulation of macrophages infiltrates hypertrophic adipose tissue and is activated by free fatty acids via toll-like receptors 2 and 4 and JNK-dependent pathways. J Biol Chem 282:35279–35292, 2007.
15. Nguyen MT, Satoh H, Favelyukis S, Babendure JL, Imamura T, Sbodio JI, Zalevsky J, Dahiyat BI, Chi NW, Olefsky JM. JNK and tumor necrosis factor-alpha mediate free fatty acid-induced insulin resistance in 3T3-L1 adipocytes. J Biol Chem 280:35361–35371, 2005.
16. Takeuchi O, Hoshino K, Kawai T, Sanjo H, Takada H, Ogawa T, Takeda K, Akira S. Differential roles of TLR2 and TLR4 in recognition of gram-negative and gram-positive bacterial cell wall components. Immunity 11:443–451, 1999.
17. MacPherson LJ, Bayburt EK, Capparelli MP, Carroll BJ, Goldstein R, Justice MR, Zhu L, Hu S, Melton RA, Fryer L, Goldberg RL, Doughty JR, Spirito S, Blancuzzi V, Wilson D, O'Byrne EM, Ganu V, Parker DT. Discovery of CGS 27023A, a non-peptidic, potent, and orally active stromelysin inhibitor that blocks cartilage degradation in rabbits. J Med Chem 40:2525–2532, 1997.
18. Kim YS, Kim SS, Cho JJ, Choi DH, Hwang O, Shin DH, Chun HS, Beal MF, Joh TH. Matrix metalloproteinase-3: a novel signaling proteinase from apoptotic neuronal cells that activates microglia. J Neurosci 25:3701–3711, 2005.
19. Bohnenkamp HR, Papazisis KT, Burchell JM, Taylor-Papadimitriou J. Synergism of toll-like receptor-induced interleukin-12p70 secretion by monocyte-derived dendritic cells is mediated through p38 MAPK and lowers the threshold of T-helper cell type 1 responses. Cell Immunol 247:72–84, 2007.
20. Weisberg SP, McCann D, Desai M, Rosenbaum M, Leibel RL, Ferrante AW Jr. Obesity is associated with macrophage accumulation in adipose tissue. J Clin Invest 112:1796–1808, 2003.
21. Xu H, Barnes GT, Yang Q, Tan G, Yang D, Chou CJ, *et al*. Chronic inflammation in fat plays a crucial role in the development of obesity-related insulin resistance. J Clin Invest 112:1821–1830, 2003.
22. Cho ML, Ju JH, Kim HR, Oh HJ, Kang CM, Jhun JY, Lee SY, Park MK, Min JK, Park SH, Lee SH, Kim HY. Toll-like receptor 2 ligand mediates the upregulation of angiogenic factor, vascular endothelial growth factor and interleukin-8/CXCL8 in human rheumatoid synovial fibroblasts. Immunol Lett 108:121–128, 2007.
23. Rega G, Kaun C, Demyanets S, Pfaffenberger S, Rychli K, Hohensinner PJ, Kastl SP, Speidl WS, Weiss TW, Breuss JM, Furnkranz A, Uhrin P, Zaujec J, Zilberfarb V, Frey M, Roehle R, Maurer G, Huber K, Wojta J. Vascular endothelial growth factor is induced by the inflammatory cytokines interleukin-6 and oncostatin m in human adipose tissue in vitro and in murine adipose tissue in vivo. Arterioscler Thromb Vasc Biol 27:1587–1595, 2007.
24. Wang B, Wood IS, Trayhurn P. Dysregulation of the expression and secretion of inflammation-related adipokines by hypoxia in human adipocytes. Pflugers Arch 455:479–492, 2007.

International Journal of Obesity (2008) 32, 902–911
 0307-0565/08 $30.00
www.nature.com/ijo

ORIGINAL ARTICLE

Macrophages regulate tumor necrosis factor-α expression in adipocytes through the secretion of matrix metalloproteinase-3

H Unoki[1,4], H Bujo[2], M Jiang[2], T Kawamura[3], K Murakami[3] and Y Saito[3]

[1]*Division of Applied Translational Research, Chiba University Graduate School of Medicine, Chiba, Japan;* [2]*Department of Genome Research and Clinical Application, Chiba University Graduate School of Medicine, Chiba, Japan and* [3]*Department of Clinical Cell Biology, Chiba University Graduate School of Medicine, Chiba, Japan*

Objective: Adipocytes accumulated in the visceral area change their function to induce tumor necrosis factor-α (TNF-α) secretion with concomitant matrix metalloproteinase (MMP)-3 induction in mice. This study was performed to clarify the role of macrophages (Mϕ)-secreted MMP on the functional changes in adipocytes using a culture system.
Design: Cultures of 3T3-L1 adipocytes with THP-1 Mϕ or the Mϕ-conditioned medium were used to investigate the role of Mϕ-MMP on the TNF-α gene in 3T3-L1 adipocytes by the addition of MMP inhibitors. For animal experiments, male C57BL/6J mice were rendered insulin resistant by feeding a high-fat diet, and the expression of an Mϕ marker F4/80, and MMP-3 genes in mesenteric and subcutaneous fat tissue specimens were examined.
Results: Mϕ-conditioned media (Mϕ-CM) increased the levels of TNF-α mRNA expression in 3T3-L1 adipocytes, and these adipocyte responses were abolished by treatment with GM6001, a broad-spectrum MMP inhibitor, or NNGH (*N*-isobutyl-*N*-(4-methoxyphenylsulfonyl)-glycylhydroxamic acid), an MMP-3 inhibitor. The activated form of MMP-3 enhanced glycerol release as well as TNF-α protein secretion from 3T3-L1 adipocytes. The incubation of adipocytes with MMP-3 inhibited insulin-induced glucose uptake in adipocytes. Furthermore, a high-fat intake increased the expression of MMP-3, decreased the insulin-induced glucose uptake of adipocytes and induced expression of F4/80 in mesenteric fat tissue of C57BL/6 mice.
Conclusion: Mϕ may cause a pathological link with surrounding adipocytes through the secretion of MMP-3 followed by TNF-α expression in adipocytes in visceral fat tissue.
International Journal of Obesity (2008) 32, 902–911; doi:10.1038/ijo.2008.7; published online 19 February 2008

Keywords: macrophage; matrix metalloproteinase-3; tumor necrosis factor-α; adipocyte; insulin resistance

Introduction

Disturbed insulin sensitivity plays an important role in the accumulation of various metabolic disorders, and has been recognized as 'metabolic syndrome'.[1,2] In accordance with the clinical significance of evaluation of visceral fat accumulation in metabolic syndrome, it has become evident that visceral fat has direct interaction with other tissues, such as muscles, liver or vessel walls, through the secretion of several molecules regulating the insulin sensitivity in tissues.[3,4] The transplantation of cultured cells into the intramesenteric space of mature mice has been established as an adequate mode for the analyses of the interaction between visceral fat and insulin sensitivity.[5] The mice with transplanted cultured adipocytes showed that visceral fat, and not subcutaneous fat, secretes the tumor necrosis factor-α (TNF-α), and the secreted molecules actually disturb the insulin sensitivity based on the decreased insulin action in tissues.[5] The accumulated visceral fat caused drastic changes in expression of matrix metalloproteinase (MMP) family genes, among which MMP-3 potentiated free fatty acid-induced TNF-α secretion from adipocytes.[6] Therefore, the MMP-3 activity in visceral fat seems to be directly linked to cytokine expression in adipocytes.

There is an infiltration of macrophages (Mϕ) in the accumulated fat tissues, and active Mϕ cause a pathological inter-relationship with surrounding adipocytes in visceral fat, which leads to the progression of insulin resistance.[7]

Correspondence: Dr H Bujo, Department of Genome Research and Clinical Application, Chiba University Graduate School of Medicine, 1-8-1 Inohana, Chuo-ku, Chiba 260-8670, Japan.
E-mail: hbujo@faculty.chiba-u.jp
[4]Current address: Laboratory for Diabetic Nephropathy, SNP Research Center, The Institute of Physical and Chemical Research, Kanagawa 230-0045, Japan.
Received 11 August 2007; revised 28 December 2007; accepted 7 January 2008; published online 19 February 2008

A variety of inflammatory bioactive molecules plays an important role in pathological interaction between Mϕ and adipocytes in visceral fat.[8–14] An overexpression of monocyte chemoattractant protein (MCP)-1 in adipose tissues causes macrophage recruitment and insulin resistance in mice.[10,11] TNF-α secretion is highly related to the free fatty acid (FFA)-induced inflammatory changes in both adipocytes and Mϕ.[12–15] The peroxisome proliferator-activated receptor activation in Mϕ is able to regulate the FFA-induced TNF-α secretion from adipocytes.[16]

The present study was designed to identify the role of MMP-3 in the interaction between Mϕ and adipocytes for TNF-α gene induction. Conditioned media from Mϕ (Mϕ-CM) increased the TNF-α mRNA expression in adipocytes. The induced levels of TNF-α mRNA were largely abolished by treatment with GM6001, a broad-spectrum MMP inhibitor, or *N*-isobutyl-*N*-(4-methoxyphenylsulfonyl)-glycylhydroxamic acid (NNGH), an MMP-3 inhibitor. The active form of MMP-3 enhanced release of TNF-α and glycerol from 3T3-L1 adipocytes, and inhibited insulin-induced glucose uptake into the cells. The MMP-3 expression in Mϕ, in addition to adipocytes, is potentially important for the development of a pathological link between Mϕ and adipocytes through TNF-α secretion in visceral fat tissue.

Methods

Cell culture and preparation of Mϕ conditioned media

3T3-L1 cells (American Type Culture Collection, Manassas, VA, USA) were cultured and differentiated into adipocytes as described previously.[16] The human monocytic cell line THP-1 (American Type Culture Collection) was cultured in RPMI 1640 supplemented with l-glutamine (GibcoBRL, Tokyo, Japan) penicillin/streptomycin (100 U per 100 mg ml^{-1}; GibcoBRL) and 10% fetal bovine serum (GibcoBRL, medium A). To allow the monocytes to differentiate into adherent macrophages, THP-1 cells were washed in phosphate-buffered saline (calcium- and magnesium-free; GibcoBRL, buffer A) and resuspended in fresh medium A containing phorbol 12-myristate-13-acetate (50 ng ml^{-1} PMA; Sigma, St Louis, MO, USA) for 3 days (at day 0), and were incubated for 3 more days in Dulbecco's modified Eagle's medium (DMEM) supplemented with 2% bovine serum albumin (BSA). At day 3, the culture media were collected, centrifuged and stored as Mϕ-CM. Control CM were prepared by incubating the THP-1 cells with DMEM supplemented with 2% BSA for 3 days (THP1-CM). Mϕ-CM and THP1-CM were stored at −80 °C until use. The differentiation of THP1 to mature Mϕ was evaluated by the quantification of CD11b and CD68 mRNA levels using real-time PCR. The differentiated macrophages with CD11b and CD68 mRNA levels of more than two fold greater than those in THP-1 were used for further experiments. Co-culture of adipocytes and Mϕ was performed using transwell inserts with 0.4-μm porous membrane (Becton Dickinson, Franklin Lakes, NJ, USA) to separate adipocytes from Mϕ. To determine the role of Mϕ-secreted factors on adipocyte responses, serum-starved 3T3-L1 adipocytes were incubated with Mϕ-CM or THP1-CM ranging from 10 to 50% of the final volume, for the indicated time periods. To evaluate the effects of MMP inhibition on Mϕ-CM, Mϕ-CM was treated with a broad-spectrum MMP inhibitor GM-6001, a specific peptide inhibitor of the gelatinases MMP-2 and -9, CTTHWGFTLC-decapeptide (CTT) or an MMP-3 inhibitor, NNGH (Calbiochem, San Diego, CA, USA) prior to the addition to adipocytes.

RNA preparation and quantitative real-time RT–PCR

Total RNA was isolated from cultured cells, and quantitative real-time reverse transcription (RT)–PCR was performed with an ABI 7000 sequence detection system using TaqMan Universal PCR Master Mix and Assays-on-Demand Gene Expression Assay Mix (PE Applied Biosystems, Foster City, CA, USA) described previously.[17] The quantification of a given gene, expressed as relative mRNA level compared with a control, was calculated after normalization to 18S rRNA.

Enzyme-linked immunosorbent assay

Serum-starved 3T3-L1 adipocytes were incubated with 100 μg ml^{-1} human MMP-3 (Sigma) for 1–3 days, and the culture medium was assayed for mouse TNF-α using commercial enzyme-linked immunosorbent assay (ELISA) kits (BioLegend, San Diego, CA, USA) according to the manufacturer's instructions as described previously.[16]

Glycerol release measurement

Differentiated 3T3-L1 adipocytes were incubated with DMEM supplemented with 1% FFA-free BSA for 2 days, and then treated with same medium with Mϕ-CM at 50% of volume, THP1-CM at 50% of volume or human MMP-3 at 100 μg ml^{-1}, in the absence or presence of 60 μM NNGH for 6 h. The concentrations of glycerol in the media were determined using a free glycerol determination kit (Sigma) following the manufacturer's protocol.

2-Deoxyglucose uptake assay

Differentiated 3T3-L1 adipocytes were preincubated in serum-starved DMEM with 50% Mϕ-CM, 50% THP1-CM or human MMP-3 at 100 μg ml^{-1}, in the absence or presence of 60 μM NNGH for 6 h. Single adipocytes were prepared from mesenteric or subcutaneous fat of mice, fed with high-fat or regular diet as described.[14] The cells were incubated in DMEM without serum for 2 h at 37 °C, and then either treated or not treated with 100 nM insulin for 15 min at 37 °C, as described previously.[18] After stimulation, 10 μM 2-[^{3}H]deoxyglucose was added and incubated for 5 min. Glucose uptake was stopped by the addition of ice-cold Krebs-Ringer HEPES buffer with 5 μM cytochalasin B and

25 mM glucose. The cells were washed three times with ice-cold Krebs-Ringer HEPES buffer with 25 mM glucose, and the ^{3}H-labeled radioactivity was counted using a scintillation counter (LS-6500; Beckman Coulter Inc., Fullerton, CA, USA).

Animals and animal care

Male C57BL/6J mice (Charles River, Wilmington, MA, USA) were rendered insulin resistant by feeding a high-fat diet consisting of 20% protein, 20% carbohydrate and 60% fat (Research Diet, New Brunswick, NJ, USA) starting at 8 weeks of age for 2 weeks as described previously.[14] Control mice were fed a standard diet consisting of 4.5% fat (Research Diet). Mesenteric and subcutaneous fat tissue specimens were resected, and total RNA was isolated as described previously.[14] All applicable institutional and governmental regulations concerning the ethical use of animal were followed during this research. All animal care and procedures were approved by the Animal Care Committee of Chiba University School of Medicine as described previously.

Western blot analysis

Membranes from fat tissue specimens were prepared and solubilized in solubilization buffer (200 mM Tris-maleate, pH 6.5, 2 mM $CaCl_2$, 0.5 mM PMSF, 2.5 mM leupeptin and 1% Triton X-100) as previously described.[19] The protein concentrations were determined using the BCA Protein Assay Reagent (Pierce, Rockford, IL, USA). For immunoblotting, equal amounts of membrane protein, protein extracted from pelleted beads, or concentrated media were separated by 10% SDS–PAGE after heating to 95 °C for 5 min under reducing conditions, and transferred to a nitrocellulose membrane. The blots were incubated with antibody against MMP-3 (SC-6839, 1:100 dilution), followed by peroxidase-conjugated anti-goat IgG, and then they were developed using the ECL detection reagents (Amersham Pharmacia, Piscataway, NJ, USA). The signals were quantified by densitometric scanning using the NIH image software program.

Statistical analysis

Results are presented as mean ± s.d. Statistical significance between two groups was evaluated by Student's *t*-test. Statistical significance among several groups was performed using a one-way ANOVA. A value of $P<0.05$ was considered to be significant.

Results

Effects of Mϕ-CM on TNF-α gene expression in 3T3-L1 adipocytes

3T3-L1 adipocytes were incubated with Mϕ in the transwell system to evaluate the interactions between Mϕ and adipocytes. A co-culture of adipocytes and Mϕ revealed significant induction of TNF-α gene in adipocytes relative to the control culture at 24 h (Figure 1a). The extent of changes in TNF-α mRNA expression was dependent on the number of Mϕ (data not shown). The role of Mϕ factors on TNF-α gene in adipocytes was investigated by incubating 3T3-L1 adipocytes with Mϕ-CM for 4 h. Consistent with the results in the transwell system, Mϕ-CM significantly induced expression of TNF-α mRNA in adipocytes (Figure 1b). The

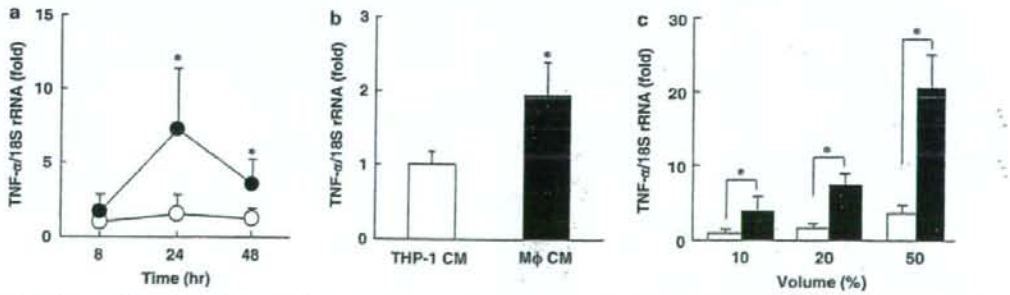

Figure 1 Mϕ-secreted factors increased the expression of tumor necrosis factor-α (TNF-α) in 3T3-L1 adipocytes. (a) Time course of the TNF-α expression in 3T3-L1 adipocytes co-cultured either with THP-1 cells (open circle) or Mϕ (filled circle). 3T3-L1 adipocytes were first seeded on the well bottom, and then THP-1 cells or THP-1 Mϕ were seeded on the permeable membrane of the insert. TNF-α mRNA levels were analyzed using quantitative real-time RT–PCR. Relative ratios of TNF-α mRNA levels in 3T3-L1 adipocytes co-cultured either with THP-1 cells or Mϕ to those co-cultured with THP-1 cells for 8 h (control) were presented. Data are expressed as mean ± s.d. ($n=4$). *$P<0.05$ in comparison to the value with THP1-CM. (b) Effects of the conditioned media of THP-1 (THP1-CM) or Mϕ cultures (Mϕ-CM) on the TNF-α gene expression in 3T3-L1 adipocytes. Serum-starved 3T3-L1 adipocytes were treated with either 10% THP1-CM or Mϕ-CM for 4 h. TNF-α mRNA levels in 3T3-L1 adipocytes were analyzed using quantitative real-time RT–PCR. The relative ratios of TNF-α mRNA levels in 3T3-L1 adipocytes with Mϕ-CM to those with THP1-CM (control) were presented. Data are expressed as mean ± s.d. ($n=4$). *$P<0.05$ in comparison to the value of the control with THP1-CM. (c) Dose-dependent effect of THP1-CM or Mϕ-CM on TNF-α gene expression in 3T3-L1 adipocytes. The TNF-α mRNA levels in 3T3-L1 adipocytes were analyzed using quantitative real-time RT–PCR. Relative ratios of TNF-α mRNA levels to those with THP1-CM at 10% of volume (control) were presented. Data are expressed as mean ± s.d. ($n=4$). *$P<0.05$.

induction of mRNA for TNF-α was 1.9-fold after 4 h of incubation with Mϕ-CM in comparison to that in control. Mϕ-CM dose-dependently increased TNF-α mRNA expression at the concentrations from 10 to 50% (Figure 1c). There were no obvious changes in the morphology of the adipocytes, and there was no apparent toxicity with either Mϕ-CM or THP1-CM (data not shown).

Role of Mϕ-derived factors in induction of TNF-α mRNA in adipocytes

The expression of the MMP-3 gene is one of most induced genes in accumulated visceral fat tissues, and MMP-3 induces the TNF-α secretion from adipocytes.[6] To explore the molecular mechanisms of the above observed interaction between Mϕ and adipocytes, the role of MMP secreted from Mϕ in the induction of TNF-α mRNA was investigated in adipocytes. The expression of MMP genes significantly increased in Mϕ in comparison to those in THP-1 cells (Figure 2). Among them, MMP-9 was most induced gene in Mϕ (199-fold). The expression of MMP-3 and -12 genes was hardly detected in THP-1 cells. These results raise the possibility that Mϕ-secreted MMP enhances the expression of the TNF-α gene in 3T3-L1 adipocytes in co-culture system. Mϕ-CM treated with various types of MMP inhibitors was added to 3T3-L1 adipocytes to examine the changes of TNF-α gene expression in 3T3-L1 adipocytes (Figure 3). GM6001, a broad-spectrum MMP inhibitor, markedly altered

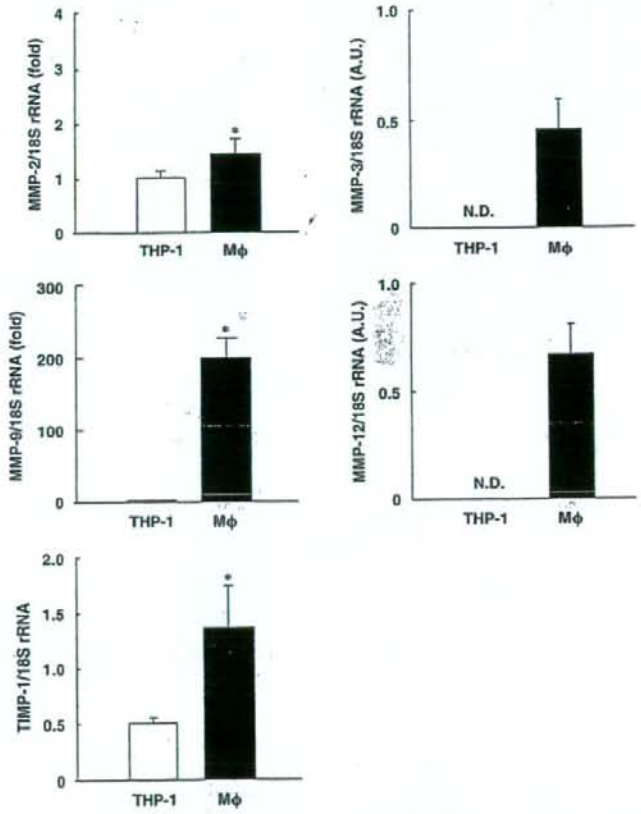

Figure 2 The expression of matrix metalloproteinase (MMP) family genes was induced in Mϕ. THP-1 cells were differentiated into Mϕ by incubating PMA for 72 h. MMP-2, MMP-3, MMP-9, MMP-12 and TIMP-1 mRNA levels were analyzed using quantitative real-time RT–PCR. Relative ratios of mRNA levels in Mϕ to those in THP-1 cells (control) or absolute mRNA levels were presented. Data are expressed as mean ± s.d. ($n = 6$). *$P < 0.05$ in comparison to the value of the control with THP-1 cells. N.D., not detected.

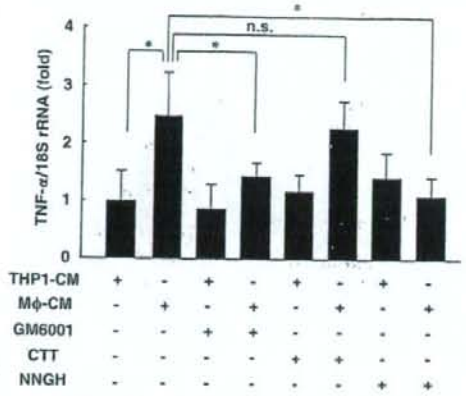

Figure 3 Effect of the inhibition of matrix metalloproteinase (MMP) activity on Mϕ-CM-induced tumor necrosis factor-α (TNF-α) gene expression in adipocytes. Serum-starved 3T3-L1 adipocytes were treated with THP-1-CM or Mϕ-CM in the absence or presence of 10 μM GM6001, 85 μM CTT or 60 μM NNGH for 4 h. the TNF-α mRNA levels were analyzed using quantitative real-time RT–PCR. Relative ratios of the TNF-α mRNA levels in 3T3-L1 adipocytes to those with THP1-CM (control) were presented. Data are expressed as mean ± s.d. ($n=4$). *$P<0.05$. n.s., not significant.

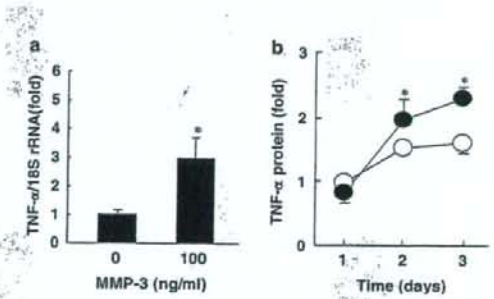

Figure 4 Matrix metalloproteinase (MMP)-3 induced the tumor necrosis factor-α (TNF-α) mRNA and protein expression in 3T3-L1 adipocytes. (a) Serum-starved 3T3-L1 adipocytes were treated with the active form of MMP-3 (100 ng ml^{-1}) for 8 h. The TNF-α mRNA levels were analyzed using quantitative real-time RT–PCR. Relative ratios of the TNF-α mRNA levels to those without MMP-3 (control) were presented. Data are expressed as mean ± s.d. ($n=6$). *$P<0.05$ compared to the value of the control. (b) Serum-starved 3T3-L1 adipocytes were treated with MMP-3 for 1–3 days. TNF-α protein concentrations in conditioned media were analyzed using an ELISA. Relative ratios of TNF-α concentration with those in the absence of MMP-3 for a day (control) were presented. Data are expressed as mean ± s.d. ($n=6$). *$P<0.05$ in comparison to the value without MMP-3.

the stimulatory effects of Mϕ-CM on the gene expression of TNF-α (−42%). The gelatinases inhibitor, CTT and an MMP-3 inhibitor, NNGH were used to determine the role of the gelatinases (MMP-2 and -9) and MMP-3 on the TNF-α gene expression in 3T3-L1 adipocytes. The stimulatory effect of Mϕ-CM on the TNF-α gene expression was not significantly inhibited by CTT treatment. In contrast, the induction of TNF-α by Mϕ-CM was markedly inhibited by NNGH treatment (−56%), suggesting an important role for MMP-3 in the adipocyte function. To determine if MMP-3 is the soluble mediator causing TNF-α induction in adipocytes, 3T3-L1 adipocytes were treated with activated MMP-3, and TNF-α mRNA expression and release were measured. MMP-3 treatment significantly increased TNF-α mRNA expression by 3.2-fold (Figure 4a), and the increases were also detected after 50–200 ng ml^{-1} MMP-3 treatments for 8 h (data not shown). Figure 4b shows that MMP-3 treatment (100 ng ml^{-1}) increased TNF-α secretion in a time-dependent manner.

Active MMP-3 induces lipolysis, and reduces insulin-induced glucose incorporation in 3T3-L1 adipocytes

In order to determine the role of Mϕ-derived MMP-3 in the functional changes of adipocytes to induce the TNF-α mRNA expression in adipocytes, the effect of MMP-3 on the lipolysis of 3T3-L1 adipocyte was analyzed (Figure 5a). The glycerol release was significantly increased in the media of